JOURNAL OF VIROLOGY, Sept. 2011, p. 8556–8568 Vol. 85, No. 17
0022-538X/11/$12.00 doi:10.1128/JVI.00146-11

Hepatitis C Virus Infection Promotes Hepatic Gluconeogenesis through an NS5A-Mediated, FoxO1-Dependent Pathway▽

Lin Deng,[1] Ikuo Shoji,[1] Wataru Ogawa,[2] Shusaku Kaneda,[1] Tomoyoshi Soga,[3] Da-peng Jiang,[1] Yoshi-Hiro Ide,[1] and Hak Hotta[1]*

Division of Microbiology, Center for Infectious Diseases,[1] and Division of Diabetes, Metabolism and Endocrinology,[2] Kobe University Graduate School of Medicine, 7-5-1 Kusunoki-cho, Chuo-ku, Kobe 650-0017, Japan, and Institute for Advanced Biosciences, Keio University, 246-2 Mizukami, Kakuganji, Tsuruoka, Yamagata 997-0052, Japan[3]

Received 21 January 2011/Accepted 7 June 2011

Chronic hepatitis C virus (HCV) infection is often associated with type 2 diabetes. However, the precise mechanism underlying this association is still unclear. Here, using Huh-7.5 cells either harboring HCV-1b RNA replicons or infected with HCV-2a, we showed that HCV transcriptionally upregulated the genes for phosphoenolpyruvate carboxykinase (PEPCK) and glucose 6-phosphatase (G6Pase), the rate-limiting enzymes for hepatic gluconeogenesis. In this way, HCV enhanced the cellular production of glucose 6-phosphate (G6P) and glucose. PEPCK and G6Pase gene expressions are controlled by the transcription factor forkhead box O1 (FoxO1). We observed that although neither the mRNA levels nor the protein levels of FoxO1 expression were affected by HCV, the level of phosphorylation of FoxO1 at Ser319 was markedly diminished in HCV-infected cells compared to the control cells, resulting in an increased nuclear accumulation of FoxO1, which is essential for sustaining its transcriptional activity. It was unlikely that the decreased level of FoxO1 phosphorylation was mediated through Akt inactivation, as we observed an increased phosphorylation of Akt at Ser473 in HCV-infected cells compared to control cells. By using specific inhibitors of c-Jun N-terminal kinase (JNK) and reactive oxygen species (ROS), we demonstrated that HCV infection induced JNK activation via increased mitochondrial ROS production, resulting in decreased FoxO1 phosphorylation, FoxO1 nuclear accumulation, and, eventually, increased glucose production. We also found that HCV NS5A mediated increased ROS production and JNK activation, which is directly linked with the FoxO1-dependent increased gluconeogenesis. Taken together, these observations suggest that HCV promotes hepatic gluconeogenesis through an NS5A-mediated, FoxO1-dependent pathway.

Hepatitis C virus (HCV) is a small, enveloped RNA virus that belongs to the genus *Hepacivirus* of the family *Flaviviridae*, and the molecular mechanisms underlying its viral replication are currently being unraveled (40). The HCV genome encodes a single polyprotein of about 3,000 amino acids, which is cleaved by host and viral proteases to generate at least 10 viral proteins, such as core, envelope 1 (E1), E2, p7, NS2, NS3, NS4A, NS4B, NS5A, and NS5B. HCV can be classified into seven genotypes, with each genotype further classified into a number of subtypes, such as HCV-1a and HCV-1b (18, 24, 59).

HCV infects more than 120 million people worldwide (57). Persistent HCV infection causes not only liver diseases (chronic hepatitis, liver cirrhosis, and hepatocellular carcinoma) but also extrahepatic manifestations, such as type 2 diabetes (2, 11, 20, 23). While it is known that liver cirrhosis impairs the glucose metabolism of the liver, there are some reports showing that HCV-infected patients over 40 years of age have an increased risk of type 2 diabetes compared with individuals without HCV infection (43). In addition, insulin receptor substrate 1 (IRS-1)/phosphatidylinositol 3-kinase (PI3-kinase) signaling was more impaired in HCV-infected patients than in non-HCV-infected controls (3). These studies imply that HCV infection may directly predispose the host toward type 2 diabetes. However, the precise mechanisms are poorly understood.

Hepatocytes play an important role in maintaining plasma glucose homeostasis by adjusting the balance between hepatic glucose production and utilization via the gluconeogenic and glycolytic pathways, respectively. It was proposed previously that increased hepatic glucose production is a major feature of type 2 diabetes (13). It is also known that hyperglycemia and the subsequent development of type 2 diabetes mellitus result, at least in part, from impaired insulin signaling together with elevated glucagon levels (5, 19). Hepatic glucose production and utilization, physiologically opposed cascades, are regulated, at least in part, at the transcriptional level of the glucose 6-phosphatase (G6Pase) and glucokinase (GK) genes, which catalyze the last and the first rate-limiting steps in gluconeogenesis and glycolysis, respectively. A number of studies have shown that fasting/feeding (or hormones) controls the transcription of these two enzymes in the opposite directions. G6Pase transcription is negatively regulated by insulin or feeding and is markedly increased in a fasting state (62). On the other hand, GK transcription is positively regulated by insulin or feeding and markedly decreased in a fasting state (33). It has also been reported that the gene expressions of gluconeogenic and glycolytic enzymes, such as G6Pase, GK, and phosphoenolpyruvate carboxykinase (PEPCK), another rate-limiting enzyme for hepatic gluconeogenesis, are regulated by certain

* Corresponding author. Mailing address: Division of Microbiology, Center for Infectious Disease, Kobe University Graduate School of Medicine, 7-5-1 Kusunoki-cho, Chuo-ku, Kobe 650-0017, Japan. Phone: 81-78-382-5500. Fax: 81-78-382-5519. E-mail: hotta@kobe-u.ac.jp.

▽ Published ahead of print on 22 June 2011.

TABLE 1. Sequences and positions of primers used in this study

Gene (GenBank accession no.)	Primer	Positions	PCR product (bp)
GK (M69051)	5′-GCCTCCCAAAGCATCTACCTC-3′ 5′-GCTCCACTGCCCCTCCTCACC-3′	119–139 562–542	444
G6Pase (U01120)	5′-CCTGGGGCTGGCTCTCAACTC-3′ 5′-AATAGTAGTCCTCCTCAATCC-3′	889–909 1197–1177	309
PEPCK (BC023978)	5′-CCAGGCAGTGAGGGAGTTTCT-3′ 5′-ACTGTGTCTCTTTGCTCTTGG-3′	210–230 426–406	217
FoxO1 (NM_002915)	5′-GAGGGTTAGTGAGCAGGTTAC-3′ 5′-AGTCCTTATCTACAGCAGCAC-3′	2352–2372 2568–2548	217
HCV NS5A (JF343793)	5′-AGACGTATTGAGGTCCATGC-3′ 5′-CCGCAGCGACGGTGCTGATAG-3′	6899–6918 7011–7031	133
β-Glucuronidase (M15182)	5′-ATCAAAAACGCAGAAAATACG-3′ 5′-ACGCAGGTGGTATCAGTCTTG-3′	1747–1767 1984–1964	238
GAPDH (NM_002046)	5′-GCCATCAATGACCCCTTCATT-3′ 5′-TCTCGCTCCTGGAAGATGG-3′	196–216 326–344	149

transcription factors, including forkhead box O1 (FoxO1) (26, 50, 54), hepatic nuclear factor 4α (HNF-4α) (26), Krüppel-like factor 15 (KLF15) (64), and cyclic AMP (cAMP) response element binding protein (CREB) (52, 56). The deregulation of the otherwise balanced control of hepatic glucose homeostasis would potentially lead to hyperglycemia and, eventually, type 2 diabetes.

In this study, by using Huh-7.5 cells harboring HCV-1b RNA replicons, i.e., either a subgenomic RNA replicon (SGR) or a full-genomic RNA replicon (FGR) (37), and cells infected with HCV-2a (14, 37, 39), we investigated the possible effects of HCV on glucose metabolism. We report here that HCV promotes hepatic gluconeogenesis, resulting in increased cellular glucose production in hepatocytes via an NS5A-mediated, FoxO1-dependent pathway.

MATERIALS AND METHODS

Cells, HCV RNA replicons, and virus. The human hepatoma-derived cell line Huh-7.5 (7) was kindly provided by C. M. Rice (Rockefeller University, New York, NY). The SGR and FGR were prepared by using pFK5B/2884Gly (41) (a kind gift from R. Bartenschlager, University of Heidelberg, Heidelberg, Germany) and pON/C-5B (31) (a kind gift from N. Kato, Okayama University, Okayama, Japan), respectively. The SGR and FGR cells are of polyclonal origin to avoid clonal variation. Plasmid pFL-J6/JFH1, which encodes the entire viral genome of a chimeric strain of HCV-2a (J6/JFH1) (39), was kindly provided by C. M. Rice. The HCV RNA genome was transcribed *in vitro* from pFL-J6/JFH1 and transfected into Huh-7.5 cells to yield infectious HCV particles, as described previously (14). A cell culture-adapted P-47 strain (9, 14) was used throughout the experiments. Virus infection was performed at a multiplicity of infection (MOI) of 2.0. Virus infectivity was measured by indirect immunofluorescence analysis, as described below, and expressed as cell-infecting units/ml. In some experiments, SGR and FGR cells, as well as HCV-infected cells at 5 days after virus infection, were treated with 1,000 IU/ml of alpha interferon (IFN) (Sigma Chemical, St. Louis, MO) for 10 days to eliminate HCV replication.

Plasmid construction. Expression plasmids for core, p7, NS2, NS3, NS3/4A, NS4A, NS4B, NS5A, and NS5B were reported elsewhere previously (15, 32).

Real-time quantitative RT-PCR. Total cellular RNA was isolated by using RNAiso reagent (Takara, Kyoto, Japan), and cDNA was generated by using a QuantiTect reverse transcription (RT) system (Qiagen, Valencia, CA). Real-time quantitative PCR was performed by using SYBR Premix Ex *Taq* (Takara) with SYBR green chemistry on an ABI Prism 7000 system (Applied Biosystems, Foster City, CA), as reported previously (37). β-Glucuronidase and GAPDH (glyceraldehyde-3-phosphate dehydrogenase) were used as internal controls. The primers used are shown in Table 1.

G6P production assay. Huh-7.5 cells seeded into a 10-cm dish at a density of 1.0×10^6 cells/dish were infected with HCV or left uninfected. At different time points after infection, the cells were washed twice with 5% mannitol solution and covered with methanol (1 ml) containing 25 μM (each) four internal standards (3-aminopyrolidine, L-methionine sulfone, trimesate, and 2-morpholinoethanesulfonic acid) for enzyme inactivation. The mixtures of methanol and cells were collected and mixed with Milli-Q water and chloroform at ratios of 2:1:2. Both the medium and cell sample solutions were then centrifuged at 20,000 × *g* for 15 min, and the aqueous layers were collected for centrifugal filtration through a 5-kDa-cutoff filter at 9,000 × *g* for 2 h. The extracted metabolites were concentrated with a centrifugal concentrator and stored at −80°C until analysis. Glucose 6-phosphate (G6P) concentrations were measured by capillary electrophoresis time-of-flight mass spectrometry (CE-TOFMS), and the results were normalized to the cell number as described previously (60, 61).

Glucose production assay. Culture medium was replaced with glucose production buffer consisting of glucose-free Dulbecco's modified Eagle's medium (DMEM) (Sigma Chemical), without phenol red, supplemented with a gluconeogenic substrate (2 mM sodium pyruvate and 20 mM sodium lactate). After 24 h of incubation, the medium was collected, and the total glucose concentration was measured by using a commercial kit (Glucose CII Test Wako; Wako Pure Chemical Industries, Osaka, Japan) and normalized to the cellular protein content. As the baseline of glucose production, glucose-free DMEM with neither sodium pyruvate nor sodium lactate was used. Glucose production via gluconeogenesis equals the total glucose production minus the baseline glucose production.

Luciferase reporter assay. The PEPCK gene promoter (position −1263/+225) and a deletion mutant (position −998/+225) were inserted into the pGL3 luciferase reporter plasmid (Promega, Madison, WI). The constructs were designated rPEPCK-P5(−1263)-pGL3basic and rPEPCK-P4(−998)-pGL3basic. pRL-CMV-Renilla (Promega), which expresses *Renilla* luciferase, was used as an internal control. Huh-7.5 cells prepared in a 12-well tissue culture plate at a density of 1.0×10^5 cells/well were transiently transfected with pRL-CMV-Renilla and rPEPCK-P5(−1263)-pGL3basic or rPEPCK-P4(−998)-pGL3basic in the presence of pEF1/NS4A, pEF1/NS5A, or a control vector (32). After 48 h, a luciferase assay was performed by using the Dual-Luciferase reporter assay system (Promega). Firefly and *Renilla* luciferase activities were measured with a Lumat LB 9501 luminometer (Berthold, Bad Wildbad, Germany). Firefly luciferase activity was normalized to *Renilla* luciferase activity for each sample.

Detection of mitochondrial ROS. Mitochondrial reactive oxygen species (ROS) production was analyzed as described previously (14). Briefly, cells seeded onto glass coverslips in a 24-well plate were incubated with 5 μM MitoSOX red (Molecular Probes, Eugene, OR) at 37°C for 10 min and then fixed with 3.7% paraformaldehyde and observed under a confocal laser scanning microscope (Carl Zeiss, Oberkochen, Germany). When needed, the fixed cells

were subjected to indirect immunofluorescence analysis to confirm HCV infection or NS5A expression, as described below.

Indirect immunofluorescence. Huh-7.5 cells seeded onto glass coverslips in a 24-well plate were infected with HCV or transfected with an NS5A expression plasmid. At 5 days postinfection (dpi) or 3 days posttransfection, the cells were fixed with 3.7% paraformaldehyde in phosphate-buffered saline (PBS) for 15 min at room temperature and permeabilized with 0.1% Triton X-100 in PBS for 15 min at room temperature. Mock-infected or empty-vector-transfected cells were similarly treated as controls for comparisons. After being washed with PBS twice, cells were consecutively stained with primary and secondary antibodies. The primary antibodies used were anti-FoxO1 rabbit monoclonal antibody (Cell Signaling Technology, Danvers, MA), anti-NS5A mouse monoclonal antibody (Chemicon International, Temecula, CA), and serum from an HCV-infected patient. Secondary antibodies used were Alexa Fluor 488-conjugated goat anti-rabbit immunoglobulin G (IgG), Alexa Fluor 594-conjugated goat anti-mouse IgG or anti-human IgG (Molecular Probes), and fluorescein isothiocyanate (FITC)-conjugated goat anti-mouse IgG or anti-human IgG (MBL, Nagoya, Japan). The stained cells were observed under a confocal laser scanning microscope (Carl Zeiss).

Cell fractionation and immunoblotting. Nuclear and cytoplasmic extracts from cells were prepared by using an NE-PER nuclear and cytoplasmic extraction reagent kit (Pierce Chemical, Rockford, IL). For immunoblotting, cells were lysed with SDS sample buffer, and equal amounts of protein were subjected to SDS-polyacrylamide gel electrophoresis and transferred onto a polyvinylidene difluoride membrane (Millipore, Bedford, MA), which was then incubated with the respective primary antibodies. The primary antibodies used were mouse monoclonal antibodies against HCV core (clone 2H9; a kind gift from T. Wakita, Department of Virology II, National Institute of Infectious Diseases, Tokyo, Japan), NS3, NS4A, NS5A, GAPDH (Chemicon), FoxO1 (Sigma Chemical), phospho-Akt (Ser473) (Cell Signaling Technology), and c-Myc (9E10; Santa Cruz Biotechnology, Santa Cruz, CA); rabbit polyclonal antibodies against phospho-FoxO1 (Ser139), Oct-1 (Santa Cruz Biotechnology), c-Jun N-terminal kinase (JNK), phospho-JNK (Thr183/Tyr185), c-Jun, phospho-c-Jun (Ser63), and Akt (Cell Signaling Technology); and goat polyclonal antibody against HSP60 (Santa Cruz Biotechnology). Horseradish peroxidase-conjugated goat anti-mouse IgG, goat anti-rabbit IgG (Molecular Probes), and donkey anti-goat IgG (Santa Cruz Biotechnology) were used to visualize the respective proteins by means of an enhanced chemiluminescence detection system (ECL; GE Healthcare, Buckinghamshire, United Kingdom).

Statistical analysis. Results were expressed as means ± standard errors of the means (SEM). Statistical significance was evaluated by analysis of variance (ANOVA) and was defined as a P value of <0.05.

RESULTS

HCV upregulates gene expression of PEPCK and G6Pase and downregulates gene expression of GK. We first examined the expression levels of the genes for the rate-limiting enzymes in hepatic gluconeogenesis, PEPCK and G6Pase, and of those for GK, which catalyzes the first step of glycolysis, by means of real-time quantitative RT-PCR analysis. We observed that the PEPCK and G6Pase genes were transcriptionally activated in SGR- and FGR-harboring cells (Fig. 1A and B, left). Similarly, the PEPCK and G6Pase genes were upregulated in HCV-infected cells in a time-dependent manner, starting from 3 or 5 days postinfection (dpi) up to 14 dpi (Fig. 1A and B, middle). On the other hand, the GK gene was transcriptionally downregulated in SGR- and FGR-harboring cells and HCV-infected cells in a time-dependent manner (Fig. 1C). It is noteworthy that the gene expressions of six glycolytic enzymes (not including GK) were observed to be upregulated in HCV-infected cells at 1 dpi (16).

When IFN treatment eliminated HCV from the cells, the observed upregulation of PEPCK and G6Pase gene expressions as well as the downregulation of GK gene expression in SGR- and FGR-harboring cells and HCV-infected cells were cancelled (Fig. 1A, B, and C, left and right). Thus, our results suggest that there was a trend toward an increase in gluconeogenesis in SGR- and FGR-harboring cells and HCV-infected cells. In subsequent studies we further examined whether or not HCV replication was correlated with gluconeogenesis.

HCV promotes cellular production of glucose and G6P. We then examined the effect of HCV on cellular glucose production. The results showed that SGR- and FGR-harboring cells and HCV-infected cells produced greater amounts of glucose than did the control cells (Fig. 2A, top and middle). IFN treatment cancelled the enhanced glucose production in SGR- and FGR-harboring cells and in HCV-infected cells (Fig. 2A, top and bottom). We also investigated the production of G6P, which is an important precursor molecule that is converted to glucose in the gluconeogenesis pathway, by means of metabolome analysis. As shown in Fig. 2B, a significantly higher level of G6P was accumulated in HCV-infected cells than in control cells. Taken together, these results indicate that HCV indeed promotes hepatic gluconeogenesis to cause hyperglycemia. In the following analyses, we examined the possible mechanisms of HCV-induced increased gluconeogenesis.

HCV suppresses FoxO1 phosphorylation at Ser319, leading to the nuclear accumulation of FoxO1. It was demonstrated previously that FoxO1 in hepatocytes enhances gluconeogenesis through the transcriptional activation of various genes, including G6Pase and PEPCK (25). To investigate the possible effects of FoxO1 on HCV-induced gluconeogenesis, we examined the gene expression levels of FoxO1 by real-time quantitative RT-PCR analysis. As shown in Fig. 3A, there was neither an upregulation nor a downregulation of FoxO1 gene expression in SGR- or FGR-harboring cells or HCV-infected cells. The FoxO1 transcription factor is controlled by various post-translational modifications, which include phosphorylation, ubiquitylation, and acetylation. The phosphorylated form of FoxO1 is exported from the nucleus and thereby loses its transcriptional function (30). We therefore examined the phosphorylation status of FoxO1 at Ser319, which is critical for FoxO1 nuclear exclusion (72). The results showed that FoxO1 phosphorylation at Ser319 was markedly suppressed in HCV-infected cells from 4 dpi up to 8 dpi, compared to that in the HCV-negative control cells (Fig. 3B, first panel), in a time-dependent manner that was roughly the inverse of the pattern observed for PEPCK and G6Pase mRNA upregulations (Fig. 1A and B) and glucose production (Fig. 2A), while the total protein expression levels of FoxO1 were unchanged (Fig. 3B, second panel). Regarding this connection, Banerjee et al. reported previously that FoxO1 phosphorylation at Ser256 was also inhibited in HCV-infected cells (4). Since FoxO1 is known to be phosphorylated by Akt so as to be exported from the nucleus and transcriptionally inactivated (38), we examined whether Akt function was suppressed through its impaired phosphorylation in HCV-infected cells. The result obtained revealed that this was not the case: Akt phosphorylation was enhanced in HCV-infected cells from 4 dpi up to 6 dpi compared with the control cells (Fig. 3B, third panel), while the total protein expression levels of Akt were comparable (Fig. 3B, fourth panel). This result is consistent with a recent observation by Burdette et al. (10) showing that the Akt phosphorylation level was elevated in HCV-infected cells. These data suggest that the observed decrease in FoxO1 phosphorylation

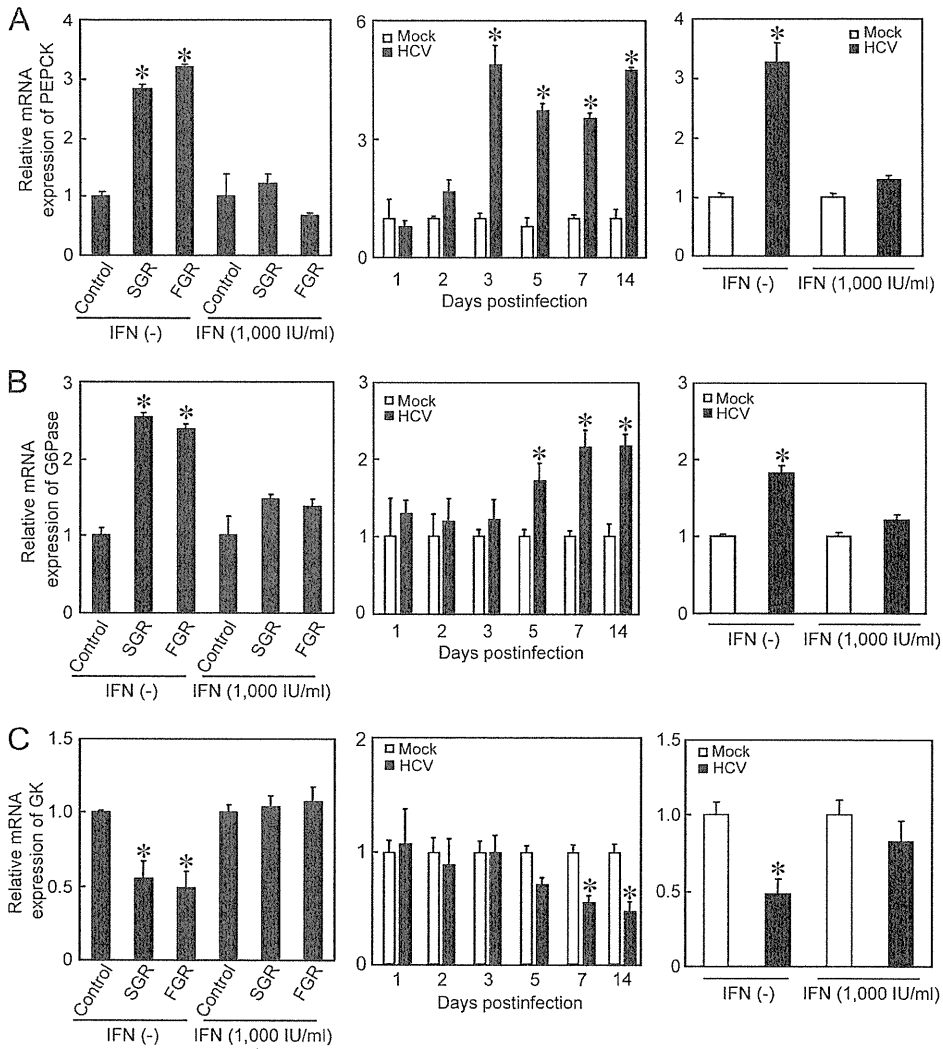

FIG. 1. HCV upregulates gene expressions of PEPCK and G6Pase and downregulates gene expression of GK. Quantitative RT-PCR analysis was performed to quantify PEPCK (A), G6Pase (B), and GK (C) mRNA expression levels in SGR- and FGR-harboring cells and HCV-infected cells (MOI = 2), and the results were normalized to β-glucuronidase mRNA expression levels. In parallel, SGR- and FGR-harboring cells and HCV-infected cells (at 5 dpi) were treated with IFN (1,000 IU/ml) for 10 days to eliminate HCV replication before being subjected to quantitative RT-PCR. Data represent means ± SEM of data from three independent experiments, and the values for the control cells were arbitrarily expressed as 1.0. *, $P < 0.01$ compared with the control.

in HCV-infected cells is caused by a mechanism independent of Akt.

Next, we tested whether HCV indeed promoted FoxO1 nuclear accumulation. The majority of FoxO1 was accumulated in the nuclear fraction in HCV-infected cells (Fig. 3C, second panel, lanes 2 and 4), whereas in control cells FoxO1 was distributed in both the nuclear and cytoplasmic fractions (lanes 1 and 3). Taken together, these results suggest that HCV suppressed FoxO1 phosphorylation, leading to the nuclear accumulation of FoxO1.

HCV-induced JNK activation is involved in the suppression of FoxO1 phosphorylation. Recent studies demonstrated that a signaling pathway that involves the stress-sensitive serine/threonine kinase JNK regulates FoxO at multiple levels (36, 66). We therefore investigated whether HCV induced JNK activation in Huh-7.5 cells. As shown in Fig. 4A, the amount of phosphorylated (activated) JNK markedly increased in HCV-infected cells in a time-dependent manner, similar to that observed for the suppression of FoxO1 phosphorylation, while the total expression levels of JNK were unchanged. As a result, c-Jun, a key substrate for JNK, was phosphorylated (activated) in HCV-infected cells but not in the mock-infected control cells. It should also be noted that the total expression levels of c-Jun in HCV-infected cells were significantly higher than those in the mock-infected control cells, suggesting that c-Jun activation through its phosphorylation stabilizes c-Jun protein expression in HCV-infected cells, as was proposed previously by Zhang et al (71).

We next sought to determine whether JNK activation was involved in the HCV-induced suppression of FoxO1 phosphorylation. HCV-infected cells at 5 days after virus infection were treated with the specific JNK inhibitor SP600125 (20 μM) (6)

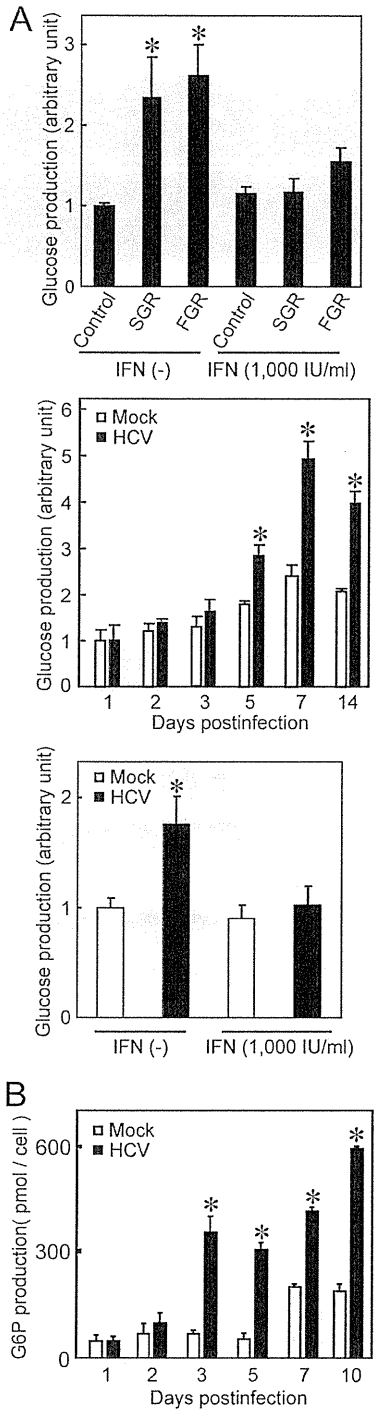

FIG. 2. HCV promotes the production of glucose and G6P. (A) Extracellular glucose production was measured in SGR- and FGR-harboring cells and HCV-infected cells (MOI = 2) and normalized to total cellular protein expression levels. In parallel, SGR- and FGR-harboring cells and HCV-infected cells (at 5 dpi) were treated with IFN (1,000 IU/ml) for 10 days to eliminate HCV replication before being subjected to glucose production analysis. Data represent means ± SEM of data from three independent experiments, and the value for the control cells was arbitrarily expressed as 1.0. *, $P < 0.01$ compared with the control. (B) Cellular G6Pase production was measured in HCV-infected cells (MOI = 2), and the results were normalized to cell numbers. Data represent means ± SEM of data from three independent experiments. *, $P < 0.01$ compared with the control.

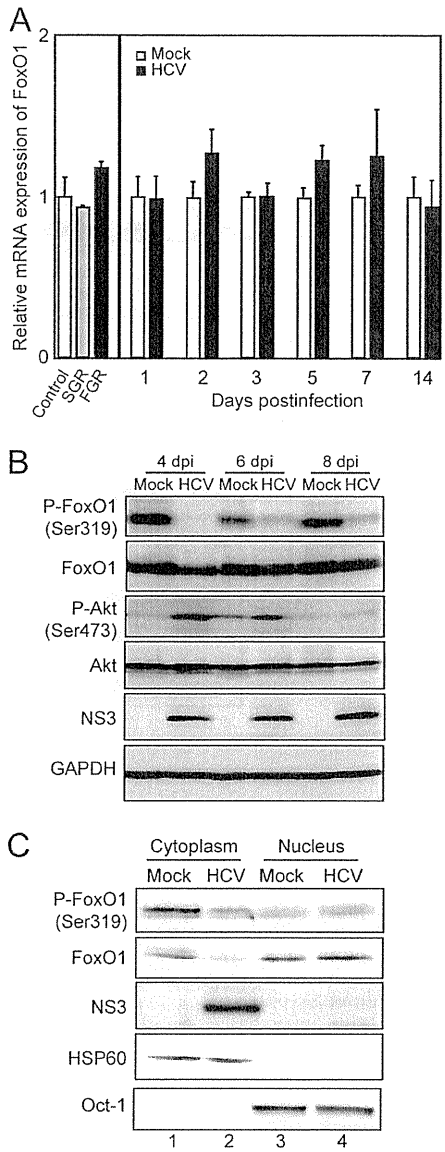

FIG. 3. HCV suppresses FoxO1 phosphorylation, leading to nuclear accumulation of FoxO1. (A) Quantitative RT-PCR analysis was performed to determine FoxO1 mRNA expression levels in SGR- and FGR-harboring cells and HCV-infected cells (MOI = 2), and expression levels were normalized to β-glucuronidase mRNA expression levels. (B) The expression levels of FoxO1, phospho-FoxO1 (Ser319) (P-FoxO1), Akt, and phospho-Akt (Ser473) were analyzed by immunoblotting of HCV-infected cells and mock-infected control cells. Blots were reprobed with antibodies recognizing NS3 and GAPDH. The amounts of GAPDH were measured as an internal control to verify equal amounts of sample loading. (C) Cytoplasmic and nuclear fractions were prepared from HCV-infected cells and mock-infected control cells at 4 dpi and were analyzed by immunoblotting using antibodies against FoxO1, phospho-FoxO1 (Ser319), NS3, Hsp60, and Oct-1. The amounts of Hsp60 and Oct-1 were measured to verify that they were equal to the amounts of cytoplasmic and nuclear fractions, respectively.

for 24 h. The catalytic JNK activity was assayed by monitoring the phosphorylation of c-Jun. As shown in Fig. 4B, SP600125 clearly prevented the phosphorylation of c-Jun and concomitantly recovered the suppression of FoxO1 phosphorylation in

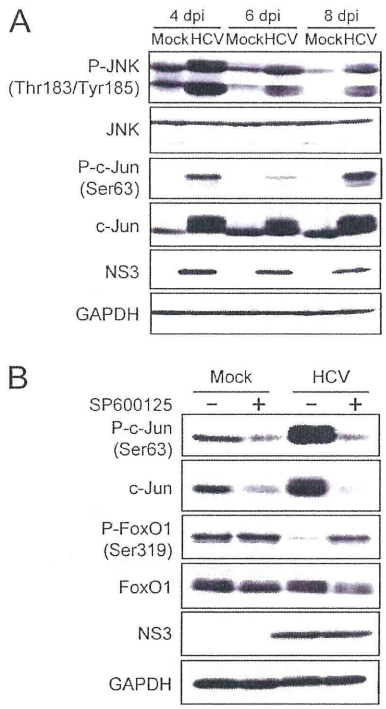

FIG. 4. HCV-induced JNK activation is required for the suppression of FoxO1 phosphorylation. (A) HCV activates the JNK/c-Jun signaling pathway. The activation (phosphorylation) of JNK (Thr183/Tyr185) and c-Jun (Ser63) in whole-cell lysates of HCV-infected cells and mock-infected control cells was analyzed by immunoblotting. Blots were reprobed with antibodies recognizing total JNK and c-Jun, NS3, and GAPDH. The amounts of GAPDH were measured as an internal control to verify equal amounts of sample loading. (B) Pretreatment with the JNK inhibitor SP600125 abrogates HCV-induced c-Jun activation and FoxO1 phosphorylation suppression. The phosphorylation of c-Jun (Ser63) and that of FoxO1 (Ser319) were analyzed by immunoblotting at 6 dpi in HCV-infected cells and mock-infected control cells with or without SP600125 pretreatment (20 μM for 24 h). Blots were reprobed with antibodies recognizing total c-Jun and FoxO1, NS3, and GAPDH. The amounts of GAPDH were measured as an internal control to verify equal amounts of sample loading.

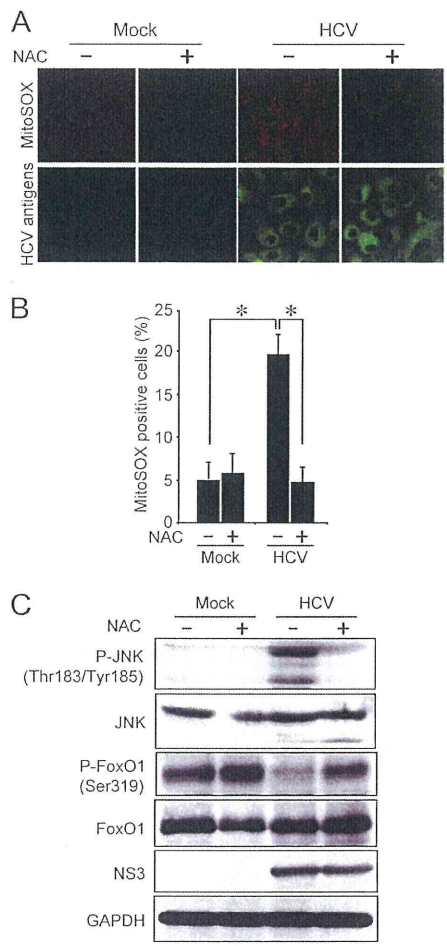

FIG. 5. HCV-induced production of mitochondrial ROS suppresses FoxO1 phosphorylation through activation of JNK. (A) Pretreatment with NAC abrogates the HCV-induced increased production of mitochondrial ROS. HCV-infected cells and mock-infected controls were pretreated with 5 mM NAC for 2 h at 6 dpi. The cells were then incubated with MitoSOX (top) and then stained for HCV antigens by using serum from an HCV-infected patient, followed by FITC-conjugated goat anti-human IgG (bottom). (B) Quantification of MitoSOX-stained cells. The percentages of cells stained with MitoSOX were determined for HCV-infected cells and mock-infected controls with or without NAC pretreatment. Data represent means ± SEM of data from two independent experiments. *, $P < 0.01$. (C) NAC pretreatment abrogates HCV-induced JNK activation and FoxO1 phosphorylation suppression. The phosphorylation of JNK (Thr183/Tyr185) and that of FoxO1 (Ser319) were analyzed by immunoblotting at 6 dpi in HCV-infected cells and mock-infected controls with or without NAC pretreatment (5 mM for 2 h). The blots were reprobed with antibodies recognizing total JNK and FoxO1, NS3, and GAPDH. The amounts of GAPDH were measured as an internal control to verify equal amounts of sample loading.

HCV-infected cells. These results suggest that HCV activates the JNK/c-Jun signaling pathway, which induces the nuclear accumulation of FoxO1 by reducing its phosphorylation status.

HCV-induced mitochondrial ROS production is involved in FoxO1 phosphorylation suppression, FoxO1 nuclear accumulation, and increased glucose production through JNK activation. We previously reported that HCV infection increases mitochondrial ROS production (14). JNK is known to be activated by ROS (35). We therefore sought to determine whether the HCV-induced increase in ROS production is an event occurring upstream of JNK activation by HCV. The pretreatment of HCV-infected cells (at 6 dpi) with 5 mM *N*-acetyl cysteine (NAC) (a general antioxidant) for 2 h significantly reduced the HCV-induced increase in ROS levels (Fig. 5A and B), as revealed by using MitoSOX, a fluorescent probe specific for superoxide that selectively accumulates in the mitochondrial compartment. As shown in Fig. 5C, NAC clearly prevented the phosphorylation of JNK and concomitantly recovered the suppression of FoxO1 phosphorylation in HCV-infected cells. These results suggest that HCV-induced ROS production is involved in JNK activation, which results in the inhibition of FoxO1 phosphorylation.

We next investigated the effects of JNK activation and ROS production on the subcellular localization of FoxO1 in HCV-infected cells by indirect immunofluorescence staining. As shown in Fig. 6A and B, FoxO1 was localized predominantly in the cytoplasm of mock-infected control cells. On the other

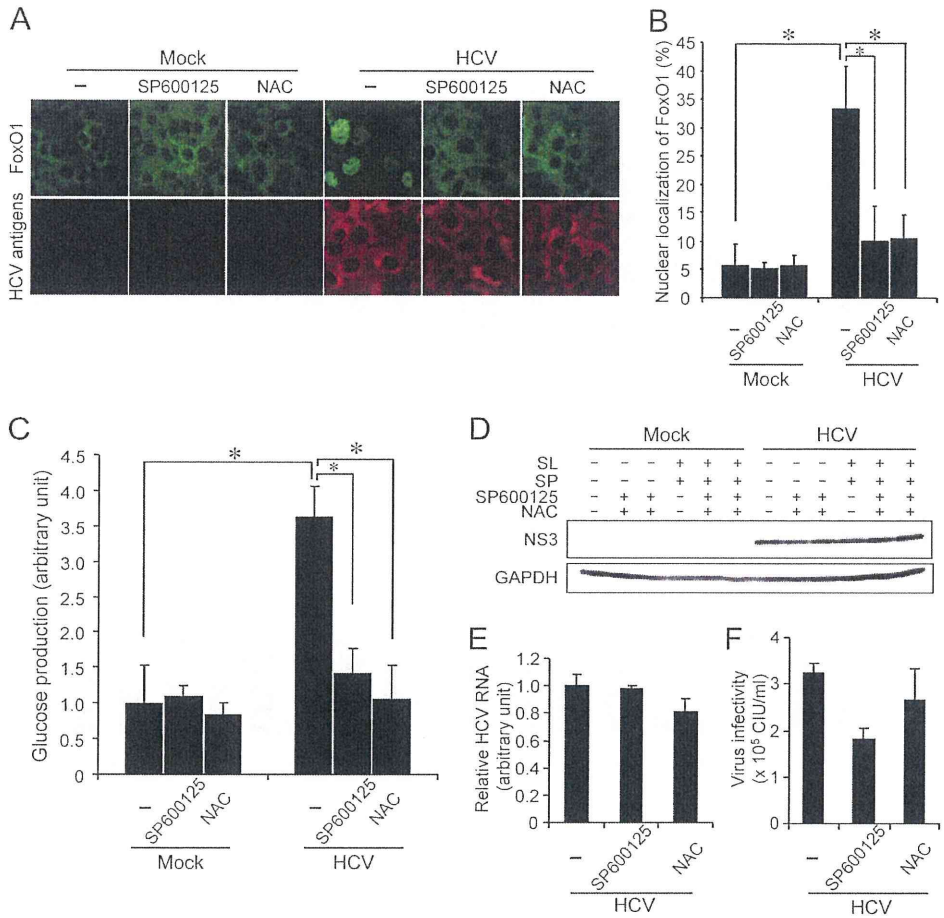

FIG. 6. HCV-induced JNK activation and ROS production are involved in FoxO1 nuclear accumulation and increased glucose production. (A) Subcellular localization of FoxO1 in HCV-infected cells and mock-infected controls with or without JNK inhibitor (SP600125 at 20 μM for 24 h) or antioxidant (NAC at 5 mM for 2 h) pretreatment at 5 dpi was examined by confocal microscopy. After fixation and permeabilization, the cells were incubated with an anti-FoxO1 rabbit monoclonal antibody followed by Alexa Fluor 488-conjugated goat anti-rabbit IgG (top) and with serum from an HCV-infected patient followed by Alexa Fluor 594-conjugated goat anti-human IgG (bottom). (B) The percentages of cells with FoxO1 nuclear localization were determined for HCV-infected cells and mock-infected controls with or without SP600125 or NAC pretreatment. Data represent means ± SEM of data from two independent experiments. *, $P < 0.01$. (C) Extracellular glucose production was measured in HCV-infected cells and mock-infected controls with or without SP600125 or NAC pretreatment at 7 dpi and normalized to total cellular protein expression levels. Data represent means ± SEM of data from two independent experiments, and the value for the control cells was arbitrarily expressed as 1.0. *, $P < 0.01$. (D) Cellular expression levels of NS3 in HCV-infected cells and mock-infected control cells with or without sodium lactate (SL), sodium pyruvate (SP), SP600125, or NAC are shown. The amounts of GAPDH were measured as an internal control to verify equal amounts of sample loading. (E) Amounts of HCV RNA were measured by quantitative RT-PCR analysis of HCV-infected cells treated with SP600125 or NAC or left untreated at 6 dpi. The amounts were normalized to GAPDH mRNA expression levels. Data represent means ± SEM of data from two independent experiments, and the value for the nontreated HCV-infected cells was arbitrarily expressed as 1.0. (F) Virus infectivity in the culture supernatants of HCV-infected cells treated with SP600125 or NAC or left untreated at 6 dpi was measured. Data represent means ± SEM of data from two independent experiments. CIU, cell-infecting units.

hand, the nuclear accumulation of FoxO1 was clearly observed in approximately 35% of HCV-infected cells at 5 dpi. The treatment of HCV-infected cells with a JNK inhibitor (SP600125 at 20 μM for 24 h) or an antioxidant (NAC at 5 mM for 2 h) significantly inhibited HCV-induced FoxO1 nuclear accumulation.

To further verify the role played by JNK activation and ROS production in HCV-induced hepatic gluconeogenesis, the glucose production in SP600125- or NAC-treated HCV-infected cells was assessed. Treatment with SP600125 or NAC significantly impaired the HCV-induced increased glucose production at 7 dpi (Fig. 6C) but did not affect the overall abundance of the HCV NS3 protein (Fig. 6D). We also examined the possible effects of SP600125 or NAC on HCV RNA replication and infectious-virus production. The results obtained revealed that treatment with SP600125 (20 μM for 24 h) or NAC (5 mM for 2 h) barely affected HCV RNA replication (Fig. 6E). On the other hand, we noted a tendency for infectious-virus production to be only slightly suppressed by SP600125 but not by NAC (Fig. 6F). A short-term inhibition of glucose production might not sufficiently affect HCV RNA replication or virus production.

Taken together, these results indicate that ROS-mediated JNK activation plays a key role in the suppression of FoxO1

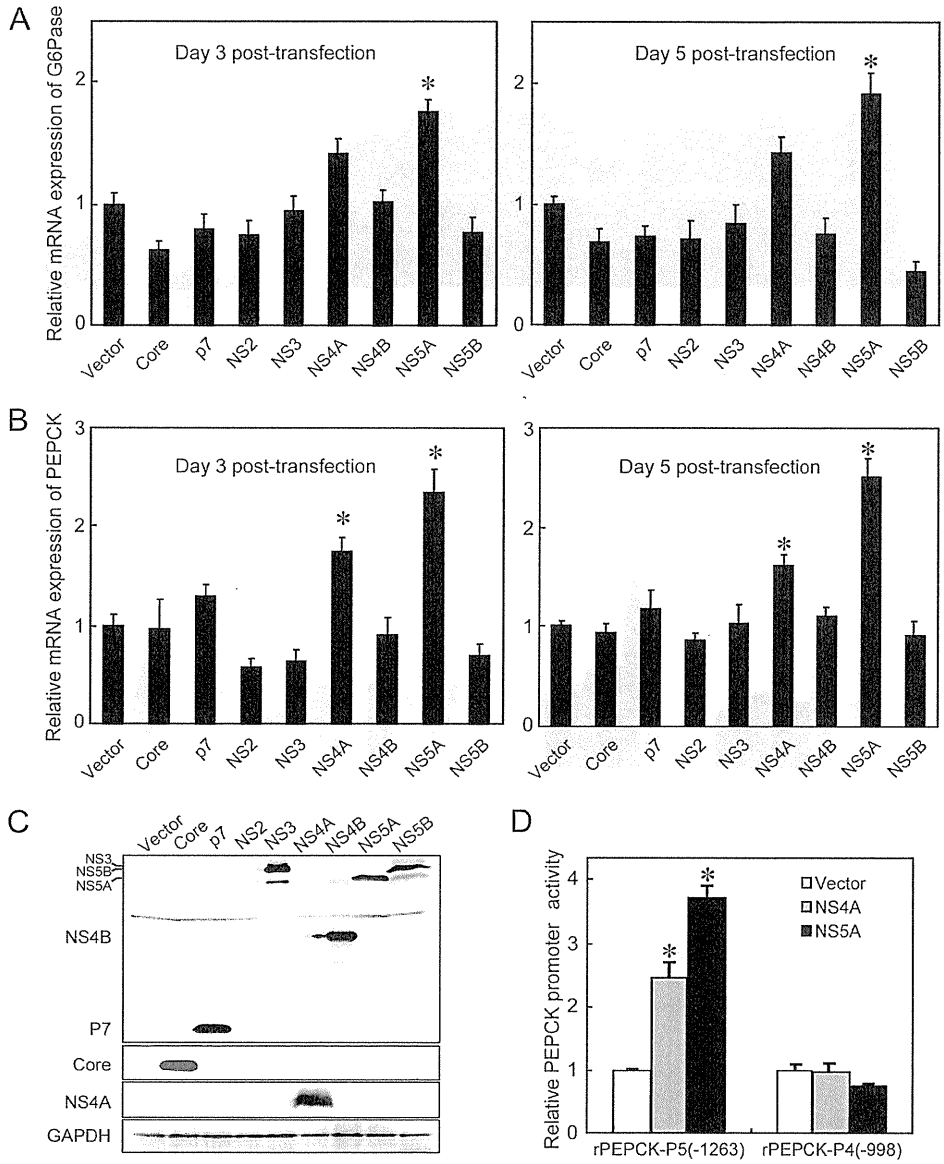

FIG. 7. HCV NS5A is involved in increased mRNA expression levels for G6Pase and PEPCK. Huh-7.5 cells were transfected with the indicated HCV viral protein expression plasmids. (A and B) At 3 and 5 days posttransfection, quantitative RT-PCR analyses of mRNA for G6Pase (A) and PEPCK (B) were conducted, and the results were normalized to β-glucuronidase mRNA expression levels. Data represent means ± SEM of data from three independent experiments, and the values for the control cells were arbitrarily expressed as 1.0. *, $P < 0.01$ compared with the control. (C) At 3 days posttransfection, the expression levels of each of the HCV proteins were examined by immunoblot analysis using antibodies against c-Myc, core, NS4A, and GAPDH. The amounts of GAPDH served as an internal control to verify equal amounts of sample loading. (D) NS5A and NS4A enhance PEPCK promoter activity. NS5A and NS4A expression plasmids were each cotransfected with rPEPCK-P5(−1263)-pGL3basic or rPEPCK-P4(−998)-pGL3basic in Huh-7.5 cells. At 48 h after transfection, the PEPCK promoter activities were measured by using a luciferase reporter assay. Data represent means ± SEM of data from three independent experiments, and the values for the control cells were arbitrarily expressed as 1.0. *, $P < 0.05$ compared with the control.

phosphorylation, the nuclear accumulation of FoxO1, and the enhancement of glucose production in HCV-infected cells.

HCV NS5A is involved in the enhancement of glucose production. To examine which HCV protein(s) is involved in the enhancement of gluconeogenesis, expression constructs of each of the HCV viral proteins were transfected into Huh-7.5 cells, and the gene expression levels of PEPCK and G6Pase were examined by real-time quantitative RT-PCR analysis. We observed that NS5A significantly promoted G6Pase gene expression (Fig. 7A). Moreover, both the NS5A and NS4A proteins significantly enhanced PEPCK gene expression at 3 and 5 days posttransfection, respectively (Fig. 7B). The expression of each of the HCV proteins except NS2 was verified by immunoblot analysis (Fig. 7C). NS2 was reported previously to be unstable and rapidly degraded by the proteasome (22).

Next, we performed a luciferase reporter assay to examine

the possible effects of NS5A and NS4A on PEPCK promoter activities. The construct rPEPCK-P5(−1263)-pGL3basic carries 1,263 bp of the PEPCK 5′-flanking region (−1263 PEPCK) and is used to monitor PEPCK promoter activity. The results demonstrated that the levels of PEPCK promoter activities were significantly higher in both NS5A- and NS4A-expressing cells than in the control cells (Fig. 7D). Interestingly, when the region of the PEPCK promoter from positions −1263 to −998 was deleted, the activation of PEPCK promoter activity in cells expressing NS5A and NS4A was abolished. These results confirmed that NS5A and NS4A activate the PEPCK promoter, leading to an increase in PEPCK mRNA expression levels. Database searches of the deleted sequence did not reveal any potential binding sequences for transcription factors (data not shown).

Recently reported data suggest that ROS production is induced in NS5A-expressing cells (17) or in hepatocytes of NS5A transgenic mice (68). We therefore sough to determine whether NS5A contributes to increased hepatic gluconeogenesis through the induction of ROS production. The NS5A expression plasmid was transfected into Huh-7.5 cells, and ROS production was assessed by MitoSOX at 3 days posttransfection. As shown in Fig. 8A and B, approximately 30% of NS5A-expressing cells displayed a much stronger signal than that observed for vector-transfected control cells.

We then examined whether NS5A mediated JNK/c-Jun activation and FoxO1 phosphorylation inhibition. The results obtained revealed that both the phosphorylation level at Ser63 and the total expression level of c-Jun were upregulated in NS5A-expressing cells compared to the control cells transfected with the vector plasmid or cells expressing the other HCV proteins (Fig. 8C and D, top two panels). Concomitantly, FoxO1 phosphorylation at Ser319 was clearly suppressed in NS5A- and NS4A-expressing cells compared to the control cells (Fig. 8C, compare lanes 6, 5, and 1, respectively, in the third panel). NS4A, a small protein of ca. 7 kDa, forms a stable complex with NS3 to function as a cofactor for NS3 serine protease and RNA helicase activities (51). We previously reported that NS4A caused mitochondrial damage when expressed alone but not when coexpressed with NS3 (47). We therefore speculated that the otherwise observed decrease in FoxO1 phosphorylation levels in NS4A-expressing cells might be canceled when NS4A is coexpressed with NS3. To verify this notion, we tested FoxO1 phosphorylation in cells coexpressing NS3 and NS4A. As had been expected, FoxO1 phosphorylation levels did not differ between NS3/4A-coexpressing cells and vector-transfected control cells (Fig. 8C, compare lanes 4 and 1, respectively).

Notably, we observed that the HCV core protein did not alter the phosphorylation status of c-Jun and FoxO1 (Fig. 8C, compare lanes 1 and 2), with the result being consistent with what was observed for gene expression levels of PEPCK and G6Pase in HCV core-expressing cells (Fig. 7A and B). These results imply that core is not primarily involved in HCV-induced increased gluconeogenesis under our experimental conditions. Similarly, other HCV nonstructural proteins, such as NS4B and NS5B, did not significantly influence the phosphorylation status of c-Jun and FoxO1 (Fig. 8D).

In order to further verify the effect of NS5A on the nuclear accumulation of FoxO1, we examined the subcellular localization of FoxO1 in NS5A-expressing cells by indirect immunofluorescence staining. As shown in Fig. 8E and F, the nuclear accumulation of FoxO1 was clearly observed for approximately 25% of NS5A-expressing cells but not the vector-transfected control. These results suggest that NS5A activates the JNK/c-Jun signaling pathway via increased ROS production, which results in the decreased phosphorylation and nuclear accumulation of FoxO1.

Finally, we examined the effects of NS5A and NS4A on glucose production. As shown in Fig. 9, the amounts of glucose were significantly increased in culture supernatants of NS5A- and NS4A-expressing cells, compared with the amounts of glucose in control cells, at 5 days posttransfection. Again, it is reasonable to assume that the observed increase in glucose production in NS4A-expressing cells might be canceled when NS4A is coexpressed with NS3.

These results collectively suggest that NS5A plays a role, at least to some extent, in the HCV-induced enhancement of hepatic gluconeogenesis.

DISCUSSION

Hepatocytes play an important role in maintaining plasma glucose homeostasis by adjusting the balance between hepatic glucose production and utilization via the gluconeogenic and glycolytic pathways, respectively. We previously reported that HCV suppresses cellular glucose uptake by downregulating the surface expression of the glucose transporters GLUT1 and GLUT2 (37). In this study, we have demonstrated that HCV promotes FoxO1-mediated hepatic gluconeogenesis, as evidenced by the increased accumulation of FoxO1 in the nucleus via the reduction of its phosphorylation status (Fig. 3 and 6A and B), which leads to increased PEPCK and G6Pase gene expression levels (Fig. 1A and B) and the subsequent upregulation of G6P and glucose production (Fig. 2). Moreover, our results indicate that HCV-induced ROS production causes JNK activation, which results in the decreased phosphorylation and nuclear accumulation of FoxO1, leading eventually to increased glucose production (Fig. 4 to 6). Our results thus suggest that FoxO1 is a prime transcription factor in the HCV-mediated progression of hepatic gluconeogenesis through an ROS/JNK-dependent mechanism, as summarized in the schema in Fig. 10. Our results also suggest that HCV NS5A plays a role in enhanced hepatic gluconeogenesis by promoting ROS production and JNK activation (Fig. 7 to 9). In line with our observations, the NS5A-mediated induction of ROS production (68) and JNK activation (49) was reported previously by other investigators.

Increasing evidence suggests that mitochondrial dysfunction is causative of insulin resistance and type 2 diabetes. Mitochondrial dysfunction causes the upregulation of PEPCK and G6Pase, leading to increased gluconeogenesis and insulin resistance (42, 46). We previously reported that HCV causes mitochondrial damage and mitochondrion-mediated apoptosis (14, 47). Our current data further support the concept that altered mitochondrial function plays a role in the development of increased glucose production in hepatocytes.

We and other groups have reported that HCV infection increases the production of mitochondrial ROS, which plays an important role in the development and progression of inflam-

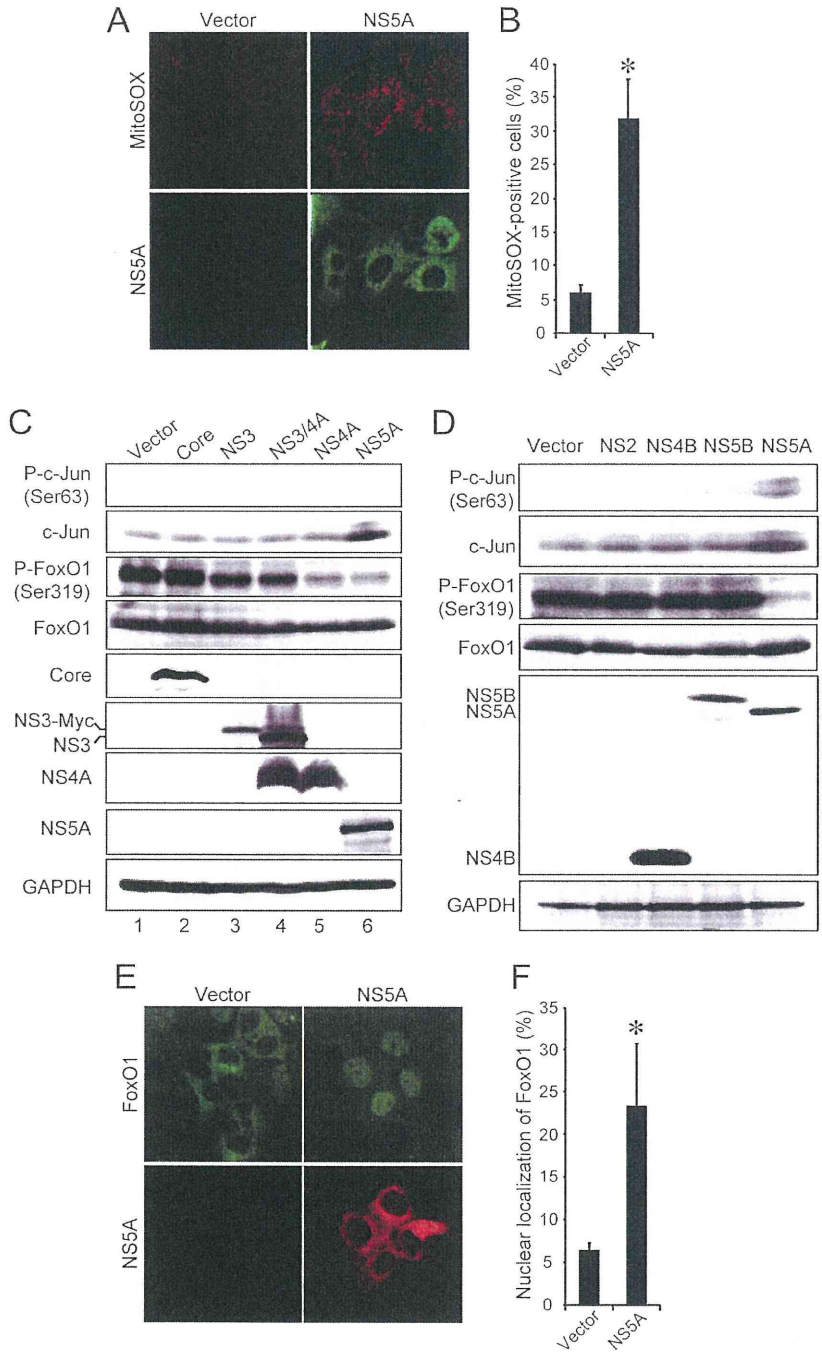

FIG. 8. HCV NS5A is involved in increased ROS production, JNK activation, FoxO1 phosphorylation suppression, and FoxO1 nuclear accumulation. (A) NS5A promotes ROS production. Huh-7.5 cells transfected with an NS5A expression plasmid or the empty control (vector) were incubated with MitoSOX (top) at 3 days posttransfection and then stained for NS5A by using anti-NS5A mouse monoclonal antibody, followed by FITC-conjugated goat anti-mouse IgG (bottom). (B) Quantification of MitoSOX-stained cells. The percentages of cells stained with MitoSOX were determined for NS5A-expressing cells and control cells. Data represent means ± SEM of data from two independent experiments. *, $P < 0.01$. (C and D) HCV NS5A activates c-Jun phosphorylation and suppresses FoxO1 phosphorylation. Huh-7.5 cells transfected with the indicated HCV viral protein expression plasmids were harvested at 3 days posttransfection, and the whole-cell lysates were subjected to immunoblot analysis using antibodies against phospho-c-Jun (Ser63), c-Jun, phospho-FoxO1 (Ser319), FoxO1, GAPDH, core, NS3, NS4A, and NS5A (C) or c-Myc (D). The amounts of GAPDH were measured as an internal control to verify equal amounts of sample loading. (E) NS5A facilitates FoxO1 nuclear accumulation. Huh-7.5 cells transfected with an NS5A expression plasmid or the empty control (vector) were fixed and permeabilized at 3 days posttransfection. The cells were incubated with an anti-FoxO1 rabbit monoclonal antibody followed by Alexa Fluor 488-conjugated goat anti-rabbit IgG (top) or with anti-NS5A mouse monoclonal antibody followed by Alexa Fluor 594-conjugated goat anti-mouse IgG (bottom). (F) The percentages of cells with a nuclear localization of FoxO1 were determined for NS5A-expressing cells and control cells. Data represent means ± SEM of data from two independent experiments. *, $P < 0.01$.

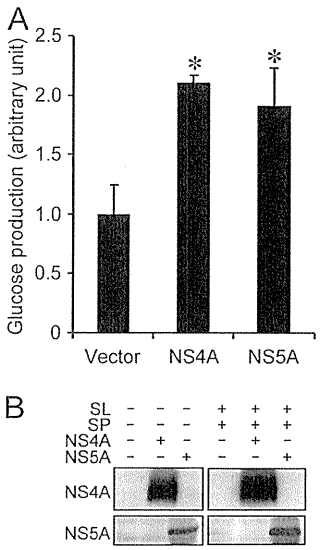

FIG. 9. HCV NS5A and NS4A enhance glucose production. (A) Huh-7.5 cells were transfected with either an NS5A or NS4A expression plasmid. At 5 days posttransfection, extracellular glucose production was measured and normalized to the total cellular protein expression level. Data represent means ± SEM of data from two independent experiments, and the values for the control cells were arbitrarily expressed as 1.0. *, $P < 0.05$ compared with the control. (B) Cellular expression levels of NS4A and NS5A in the absence and presence of sodium lactate (SL) and sodium pyruvate (SP) are shown.

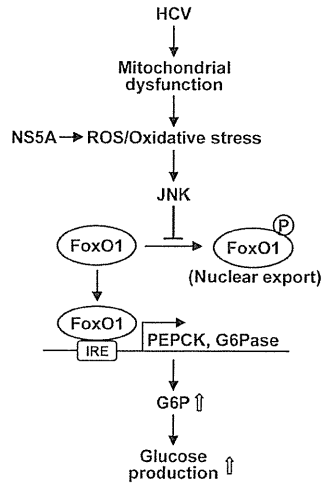

FIG. 10. Schematic representation of the HCV-dysregulated hepatic gluconeogenesis signaling pathway. HCV induces mitochondrial dysfunction (14). This results in increased ROS production and JNK activation, which induces the nuclear accumulation of FoxO1 by reducing its phosphorylation status. Consequently, PEPCK and G6Pase gene expressions are upregulated, leading to an upregulation of G6P and glucose production. NS5A plays a role in HCV-induced gluconeogenesis via the induction of ROS production. IRE, insulin response element.

matory liver disease mediated by HCV (12, 14). Increased mitochondrial ROS generation was also shown previously to be an underlying mediator of multiple forms of insulin resistance, including inflammation- or glucocorticoid-induced insulin resistance (27, 29). Moreover, a significant correlation was observed between oxidative stress and insulin resistance in patients infected with HCV genotype 1 or 2 (44). ROS have also been shown to regulate the activity of the FoxO transcription factor by posttranslational modifications, including phosphorylation (21), deacetylation (8), and ubiquitylation (67).

Although this study showed that JNK induces the nuclear accumulation of FoxO1 by reducing its phosphorylation status under oxidative stress conditions in HCV-infected cells, the precise mechanism(s) of the interplay between JNK and FoxO1 still remains to be addressed. It was reported previously that activated JNK phosphorylates IRS-1 at Ser307, which results in attenuated insulin signal transduction through the inhibition of the tyrosine phosphorylation of IRS-1 (1). Akt is a major downstream signaling protein for insulin/IRS-1 signaling and is activated through its phosphorylation on Thr308 and Ser473, the latter of which is believed to be more crucial (53). Therefore, an impairment of the insulin/IRS-1 signaling pathway should involve the downregulation of Akt phosphorylation. However, our present data showed that Akt phosphorylation on Ser473 was upregulated in HCV-infected cells at 4 and 6 dpi (Fig. 3B), suggesting that an Akt-independent pathway is involved in the JNK-mediated suppression of FoxO1 phosphorylation. Regarding this connection, it should be noted that the 14-3-3 protein, a binding partner for phosphorylated FoxO1 that mediates its nuclear export (72), is phosphorylated by JNK and that the phosphorylated 14-3-3 protein releases its binding partners, which would facilitate the nuclear accumulation of FoxO (63, 65, 70). Further studies are needed to elucidate this issue.

Another trigger that causes excessive JNK activation and insulin resistance is endoplasmic reticulum (ER) stress (28, 48). Several previous studies reported that HCV infection induces ER stress (34, 55). Under our experimental conditions, however, we did not detect significant ER stress in HCV-infected cells (14). It is thus likely that ER stress was not the primary cause of the increased gluconeogenesis in our experimental system using Huh-7.5 cells and the P-47 strain of HCV J6/JFH-1 (9, 14).

Notably, our present data showed that cells harboring the SGR or FGR and HCV-infected cells produced greater amounts of glucose than did the control cells (Fig. 2A); however, the changes in the phosphorylation status of FoxO1 and JNK in SGR- and FGR-harboring cells were not so significant compared to those in virus-infected cells (data not shown). One of the reasons for this difference is that SGR- and FGR-harboring cells were obtained through a longer cultivation in a selection medium for a month or more and that the balance of host gene induction may be somewhat different from that in virus-infected cells. Therefore, it is possible that, in addition to the JNK-FoxO1 pathway, another signaling pathway(s) is involved in the increased gluconeogenesis in SGR- and FGR-harboring cells. Studies on this issue are now under way in our laboratory.

We observed that HCV infection modulated, either positively or negatively, the transcription of the PEPCK, G6Pase, and GK genes at 3 to 5 dpi (Fig. 1). Virus infection, in general, causes dynamically changing induction and the suppression of a wide variety of host genes. For example, expression levels of certain genes, such as interferon genes, increase during an

early phase of virus infection, e.g., at 1 dpi, but return to normal levels within a few days in a cell culture system. On the other hand, the virus-infection-induced expression of other genes, such as the extracellular signal-regulated kinase (ERK) gene, remains for a prolonged period of time (data not shown). Also, some of the gene products induced in the acute phase may suppress the expression of other genes. Under these balanced conditions, it is quite possible that certain genes are induced only at a later time, e.g., 3 to 5 dpi, but not immediately after virus infection.

It was reported previously that HCV core protein-expressing transgenic mice exhibit marked insulin resistance by inhibiting IRS-1 tyrosine phosphorylation and Akt phosphorylation (45, 58). However, our present results showed that HCV NS5A, but not the core protein, was associated with increased gluconeogenesis. Moreover, it was recently reported that HCV infection significantly inhibited cellular glucose levels at 10 dpi (69), which is quite the opposite of what we observed in the present study. These results collectively suggest the possibility that multiple pathways are involved in glucose metabolism in HCV-infected cells. Also, the possible effect(s) of the dysregulation of hepatic gluconeogenesis on the HCV life cycle needs to be clarified.

In conclusion, our present results collectively suggest that HCV promotes hepatic gluconeogenesis, resulting in increased glucose production in hepatocytes via an NS5A-mediated, FoxO1-dependent pathway.

ACKNOWLEDGMENTS

We are grateful to C. M. Rice (Rockefeller University, New York, NY) for providing Huh-7.5 cells and pFL-J6/JFH1, R. Bartenschlager (University of Heidelberg, Heidelberg, Germany) for providing an HCV subgenomic RNA replicon (pFK5B/2884Gly), and N. Kato (Okayama University, Okayama, Japan) for providing an HCV full-length RNA replicon (pON/C-5B). We also thank T. Adachi (Kyoto Prefectural University of Medicine, Kyoto, Japan), K. Igarashi, K. Kashikura, and A. Suzuki (Keio University, Yamagata, Japan) for their technical assistance.

This work was supported in part by grants-in-aid for research on hepatitis from the Ministry of Health, Labor, and Welfare, Japan, and the Japan Initiative for Global Research Network on Infectious Diseases (J-GRID) program of the Ministry of Education, Culture, Sports, Science, and Technology, Japan. This study was also carried out as part of the Global Center of Excellence program of the Kobe University Graduate School of Medicine and the Science and Technology Research Partnership for Sustainable Development (SATREPS) program of the Japan Science and Technology Agency (JST) and the Japan International Cooperation Agency (JICA).

REFERENCES

1. **Aguirre, V., T. Uchida, L. Yenush, R. Davis, and M. F. White.** 2000. The c-Jun NH(2)-terminal kinase promotes insulin resistance during association with insulin receptor substrate-1 and phosphorylation of Ser(307). J. Biol. Chem. **275:**9047–9054.
2. **Alaei, M., and F. Negro.** 2008. Hepatitis C virus and glucose and lipid metabolism. Diabetes Metab. **34:**692–700.
3. **Aytug, S., D. Reich, L. E. Sapiro, D. Bernstein, and N. Begum.** 2003. Impaired IRS-1/PI3-kinase signaling in patients with HCV: a mechanism for increased prevalence of type 2 diabetes. Hepatology **38:**1384–1392.
4. **Banerjee, A., K. Meyer, B. Mazumdar, R. B. Ray, and R. Ray.** 2010. Hepatitis C virus differentially modulates activation of forkhead transcription factors and insulin-induced metabolic gene expression. J. Virol. **84:**5936–5946.
5. **Baron, A. D., L. Schaeffer, P. Shragg, and O. G. Kolterman.** 1987. Role of hyperglucagonemia in maintenance of increased rates of hepatic glucose output in type II diabetics. Diabetes **36:**274–283.
6. **Bennett, B. L., et al.** 2001. SP600125, an anthrapyrazolone inhibitor of Jun N-terminal kinase. Proc. Natl. Acad. Sci. U. S. A. **98:**13681–13686.
7. **Blight, K. J., J. A. McKeating, and C. M. Rice.** 2002. Highly permissive cell lines for subgenomic and genomic hepatitis C virus RNA replication. J. Virol. **76:**13001–13014.
8. **Brunet, A., et al.** 2004. Stress-dependent regulation of FOXO transcription factors by the SIRT1 deacetylase. Science **303:**2011–2015.
9. **Bungyoku, Y., et al.** 2009. Efficient production of infectious hepatitis C virus with adaptive mutations in cultured hepatoma cells. J. Gen. Virol. **90:**1681–1691.
10. **Burdette, D., M. Olivarez, and G. Waris.** 2010. Activation of transcription factor Nrf2 by hepatitis C virus induces the cell-survival pathway. J. Gen. Virol. **91:**681–690.
11. **Caronia, S., et al.** 1999. Further evidence for an association between non-insulin-dependent diabetes mellitus and chronic hepatitis C virus infection. Hepatology **30:**1059–1063.
12. **Choi, J., and J. H. Ou.** 2006. Mechanisms of liver injury. III. Oxidative stress in the pathogenesis of hepatitis C virus. Am. J. Physiol. Gastrointest. Liver Physiol. **290:**G847–G851.
13. **Clore, J. N., J. Stillman, and H. Sugerman.** 2000. Glucose-6-phosphatase flux in vitro is increased in type 2 diabetes. Diabetes **49:**969–974.
14. **Deng, L., et al.** 2008. Hepatitis C virus infection induces apoptosis through a Bax-triggered, mitochondrion-mediated, caspase 3-dependent pathway. J. Virol. **82:**10375–10385.
15. **Deng, L., et al.** 2006. NS3 protein of hepatitis C virus associates with the tumour suppressor p53 and inhibits its function in an NS3 sequence-dependent manner. J. Gen. Virol. **87:**1703–1713.
16. **Diamond, D. L., et al.** 2010. Temporal proteome and lipidome profiles reveal hepatitis C virus-associated reprogramming of hepatocellular metabolism and bioenergetics. PLoS Pathog. **6:**e1000719.
17. **Dionisio, N., et al.** 2009. Hepatitis C virus NS5A and core proteins induce oxidative stress-mediated calcium signalling alterations in hepatocytes. J. Hepatol. **50:**872–882.
18. **Doi, H., C. Apichartpiyakul, K. I. Ohba, M. Mizokami, and H. Hotta.** 1996. Hepatitis C virus (HCV) subtype prevalence in Chiang Mai, Thailand, and identification of novel subtypes of HCV major type 6. J. Clin. Microbiol. **34:**569–574.
19. **Dunning, B. E., and J. E. Gerich.** 2007. The role of alpha-cell dysregulation in fasting and postprandial hyperglycemia in type 2 diabetes and therapeutic implications. Endocr. Rev. **28:**253–283.
20. **Eslam, M., M. A. Khattab, and S. A. Harrison.** 2011. Insulin resistance and hepatitis C: an evolving story. Gut **60:**1139–1151.
21. **Essers, M. A., et al.** 2004. FOXO transcription factor activation by oxidative stress mediated by the small GTPase Ral and JNK. EMBO J. **23:**4802–4812.
22. **Franck, N., J. Le Seyec, C. Guguen-Guillouzo, and L. Erdtmann.** 2005. Hepatitis C virus NS2 protein is phosphorylated by the protein kinase CK2 and targeted for degradation to the proteasome. J. Virol. **79:**2700–2708.
23. **Galossi, A., R. Guarisco, L. Bellis, and C. Puoti.** 2007. Extrahepatic manifestations of chronic HCV infection. J. Gastrointestin. Liver Dis. **16:**65–73.
24. **Gottwein, J. M., et al.** 2009. Development and characterization of hepatitis C virus genotype 1-7 cell culture systems: role of CD81 and scavenger receptor class B type I and effect of antiviral drugs. Hepatology **49:**364–377.
25. **Gross, D. N., A. P. van den Heuvel, and M. J. Birnbaum.** 2008. The role of FoxO in the regulation of metabolism. Oncogene **27:**2320–2336.
26. **Hirota, K., et al.** 2008. A combination of HNF-4 and Foxo1 is required for reciprocal transcriptional regulation of glucokinase and glucose-6-phosphatase genes in response to fasting and feeding. J. Biol. Chem. **283:**32432–32441.
27. **Hoehn, K. L., et al.** 2009. Insulin resistance is a cellular antioxidant defense mechanism. Proc. Natl. Acad. Sci. U. S. A. **106:**17787–17792.
28. **Hotamisligil, G. S.** 2005. Role of endoplasmic reticulum stress and c-Jun NH2-terminal kinase pathways in inflammation and origin of obesity and diabetes. Diabetes **54**(Suppl. 2)**:**S73–S78.
29. **Houstis, N., E. D. Rosen, and E. S. Lander.** 2006. Reactive oxygen species have a causal role in multiple forms of insulin resistance. Nature **440:**944–948.
30. **Huang, H., and D. J. Tindall.** 2007. Dynamic FoxO transcription factors. J. Cell Sci. **120:**2479–2487.
31. **Ikeda, M., et al.** 2005. Efficient replication of a full-length hepatitis C virus genome, strain O, in cell culture, and development of a luciferase reporter system. Biochem. Biophys. Res. Commun. **329:**1350–1359.
32. **Inubushi, S., et al.** 2008. Hepatitis C virus NS5A protein interacts with and negatively regulates the non-receptor protein tyrosine kinase Syk. J. Gen. Virol. **89:**1231–1242.
33. **Iynedjian, P. B., et al.** 1989. Differential expression and regulation of the glucokinase gene in liver and islets of Langerhans. Proc. Natl. Acad. Sci. U. S. A. **86:**7838–7842.
34. **Joyce, M. A., et al.** 2009. HCV induces oxidative and ER stress, and sensitizes infected cells to apoptosis in SCID/Alb-uPA mice. PLoS Pathog. **5:**e1000291.
35. **Kamata, H., et al.** 2005. Reactive oxygen species promote TNFalpha-induced death and sustained JNK activation by inhibiting MAP kinase phosphatases. Cell **120:**649–661.
36. **Karpac, J., and H. Jasper.** 2009. Insulin and JNK: optimizing metabolic homeostasis and lifespan. Trends Endocrinol. Metab. **20:**100–106.
37. **Kasai, D., et al.** 2009. HCV replication suppresses cellular glucose uptake

through down-regulation of cell surface expression of glucose transporters. J. Hepatol. **50:**883–894.
38. **Kops, G. J., and B. M. Burgering.** 1999. Forkhead transcription factors: new insights into protein kinase B (c-akt) signaling. J. Mol. Med. **77:**656–665.
39. **Lindenbach, B. D., et al.** 2005. Complete replication of hepatitis C virus in cell culture. Science **309:**623–626.
40. **Lindenbach, B. D., and C. M. Rice.** 2005. Unravelling hepatitis C virus replication from genome to function. Nature **436:**933–938.
41. **Lohmann, V., F. Korner, A. Dobierzewska, and R. Bartenschlager.** 2001. Mutations in hepatitis C virus RNAs conferring cell culture adaptation. J. Virol. **75:**1437–1449.
42. **Lowell, B. B., and G. I. Shulman.** 2005. Mitochondrial dysfunction and type 2 diabetes. Science **307:**384–387.
43. **Mehta, S. H., et al.** 2000. Prevalence of type 2 diabetes mellitus among persons with hepatitis C virus infection in the United States. Ann. Intern. Med. **133:**592–599.
44. **Mitsuyoshi, H., et al.** 2008. Evidence of oxidative stress as a cofactor in the development of insulin resistance in patients with chronic hepatitis C. Hepatol. Res. **38:**348–353.
45. **Miyamoto, H., et al.** 2007. Involvement of the PA28gamma-dependent pathway in insulin resistance induced by hepatitis C virus core protein. J. Virol. **81:**1727–1735.
46. **Morino, K., K. F. Petersen, and G. I. Shulman.** 2006. Molecular mechanisms of insulin resistance in humans and their potential links with mitochondrial dysfunction. Diabetes **55**(Suppl. 2):S9–S15.
47. **Nomura-Takigawa, Y., et al.** 2006. Non-structural protein 4A of hepatitis C virus accumulates on mitochondria and renders the cells prone to undergoing mitochondria-mediated apoptosis. J. Gen. Virol. **87:**1935–1945.
48. **Ozcan, U., et al.** 2004. Endoplasmic reticulum stress links obesity, insulin action, and type 2 diabetes. Science **306:**457–461.
49. **Park, K. J., et al.** 2003. Hepatitis C virus NS5A protein modulates c-Jun N-terminal kinase through interaction with tumor necrosis factor receptor-associated factor 2. J. Biol. Chem. **278:**30711–30718.
50. **Puigserver, P., et al.** 2003. Insulin-regulated hepatic gluconeogenesis through FOXO1-PGC-1alpha interaction. Nature **423:**550–555.
51. **Reed, K. E., and C. M. Rice.** 2000. Overview of hepatitis C virus genome structure, polyprotein processing, and protein properties. Curr. Top. Microbiol. Immunol. **242:**55–84.
52. **Rozance, P. J., et al.** 2008. Chronic late-gestation hypoglycemia upregulates hepatic PEPCK associated with increased PGC1alpha mRNA and phosphorylated CREB in fetal sheep. Am. J. Physiol. Endocrinol. Metab. **294:** E365–E370.
53. **Sale, E. M., and G. J. Sale.** 2008. Protein kinase B: signalling roles and therapeutic targeting. Cell. Mol. Life Sci. **65:**113–127.
54. **Schmoll, D., et al.** 2000. Regulation of glucose-6-phosphatase gene expression by protein kinase Balpha and the forkhead transcription factor FKHR. Evidence for insulin response unit-dependent and -independent effects of insulin on promoter activity. J. Biol. Chem. **275:**36324–36333.
55. **Sekine-Osajima, Y., et al.** 2008. Development of plaque assays for hepatitis C virus-JFH1 strain and isolation of mutants with enhanced cytopathogenicity and replication capacity. Virology **371:**71–85.
56. **Seo, H. Y., et al.** 2010. Endoplasmic reticulum stress-induced activation of activating transcription factor 6 decreases cAMP-stimulated hepatic gluconeogenesis via inhibition of CREB. Endocrinology **151:**561–568.
57. **Shepard, C. W., L. Finelli, and M. J. Alter.** 2005. Global epidemiology of hepatitis C virus infection. Lancet Infect. Dis. **5:**558–567.
58. **Shintani, Y., et al.** 2004. Hepatitis C virus infection and diabetes: direct involvement of the virus in the development of insulin resistance. Gastroenterology **126:**840–848.
59. **Simmonds, P., et al.** 2005. Consensus proposals for a unified system of nomenclature of hepatitis C virus genotypes. Hepatology **42:**962–973.
60. **Soga, T., et al.** 2006. Differential metabolomics reveals ophthalmic acid as an oxidative stress biomarker indicating hepatic glutathione consumption. J. Biol. Chem. **281:**16768–16776.
61. **Soga, T., et al.** 2009. Metabolomic profiling of anionic metabolites by capillary electrophoresis mass spectrometry. Anal. Chem. **81:**6165–6174.
62. **Streeper, R. S., et al.** 1997. A multicomponent insulin response sequence mediates a strong repression of mouse glucose-6-phosphatase gene transcription by insulin. J. Biol. Chem. **272:**11698–11701.
63. **Sunayama, J., F. Tsuruta, N. Masuyama, and Y. Gotoh.** 2005. JNK antagonizes Akt-mediated survival signals by phosphorylating 14-3-3. J. Cell Biol. **170:**295–304.
64. **Takashima, M., et al.** 2010. Role of KLF15 in regulation of hepatic gluconeogenesis and metformin action. Diabetes **59:**1608–1615.
65. **Tsuruta, F., et al.** 2004. JNK promotes Bax translocation to mitochondria through phosphorylation of 14-3-3 proteins. EMBO J. **23:**1889–1899.
66. **van der Horst, A., and B. M. Burgering.** 2007. Stressing the role of FoxO proteins in lifespan and disease. Nat. Rev. Mol. Cell Biol. **8:**440–450.
67. **van der Horst, A., et al.** 2006. FOXO4 transcriptional activity is regulated by monoubiquitination and USP7/HAUSP. Nat. Cell Biol. **8:**1064–1073.
68. **Wang, A. G., et al.** 2009. Non-structural 5A protein of hepatitis C virus induces a range of liver pathology in transgenic mice. J. Pathol. **219:**253–262.
69. **Woodhouse, S. D., et al.** 2010. Transcriptome sequencing, microarray, and proteomic analyses reveal cellular and metabolic impact of hepatitis C virus infection in vitro. Hepatology **52:**443–453.
70. **Yoshida, K., T. Yamaguchi, T. Natsume, D. Kufe, and Y. Miki.** 2005. JNK phosphorylation of 14-3-3 proteins regulates nuclear targeting of c-Abl in the apoptotic response to DNA damage. Nat. Cell Biol. **7:**278–285.
71. **Zhang, S., J. Liu, G. MacGibbon, M. Dragunow, and G. J. Cooper.** 2002. Increased expression and activation of c-Jun contributes to human amylin-induced apoptosis in pancreatic islet beta-cells. J. Mol. Biol. **324:**271–285.
72. **Zhao, X., et al.** 2004. Multiple elements regulate nuclear/cytoplasmic shuttling of FOXO1: characterization of phosphorylation- and 14-3-3-dependent and -independent mechanisms. Biochem. J. **378:**839–849.

Microbiology and Immunology

Microbiol Immunol 2011; **55**: 774–782
doi:10.1111/j.1348-0421.2011.00382.x

ORIGINAL ARTICLE

Inhibition of hepatitis C virus replication through adenosine monophosphate-activated protein kinase-dependent and -independent pathways

Kenji Nakashima[1], Kenji Takeuchi[1,2], Kazuyasu Chihara[1,2], Hak Hotta[3] and Kiyonao Sada[1,2]

[1]Division of Microbiology, Department of Pathological Sciences, Faculty of Medical Sciences, [2]Organization for Life Science Advancement Programs, University of Fukui, Fukui and [3]Division of Microbiology, Center for Infectious Diseases, Kobe University Graduate School of Medicine, Kobe, Japan

ABSTRACT

Persistent infection with hepatitis C virus (HCV) is closely correlated with type 2 diabetes. In this study, replication of HCV at different glucose concentrations was investigated by using J6/JFH1-derived cell-adapted HCV in Huh-7.5 cells and the mechanism of regulation of HCV replication by AMP-activated protein kinase (AMPK) as an energy sensor of the cell analyzed. Reducing the glucose concentration in the cell culture medium from 4.5 to 1.0 g/L resulted in suppression of HCV replication, along with activation of AMPK. Whereas treatment of cells with AMPK activator 5-aminoimidazole-4-carboxamide 1-β-D-ribofuranoside (AICAR) suppressed HCV replication, compound C, a specific AMPK inhibitor, prevented AICAR's effect, suggesting that AICAR suppresses the replication of HCV by activating AMPK in Huh-7.5 cells. In contrast, compound C induced further suppression of HCV replication when the cells were cultured in low glucose concentrations or with metformin. These results suggest that low glucose concentrations and metformin have anti-HCV effects independently of AMPK activation.

Key words 5-aminoimidazole-4-carboxamide 1-β-D-ribofuranoside (AICAR), adenosine monophosphate-activated protein kinase (AMPK), diabetes, metformin.

Hepatitis C virus, which is classified within the family *Flaviviridae*, is a small enveloped virus that possesses a positive-sense single-stranded RNA genome. HCV infection proceeds to a persistent stage at a high rate, leading to cirrhosis and hepatocellular carcinoma. Despite recent advances in the development of antiviral therapies, certain patient populations are difficult to treat (1) due to host factors such as obesity, hyperglycemia and insulin resistance (2–4).

Adenosine monophosphate-activated protein kinase is a major cellular energy sensor that is activated by cellular stresses that increase intracellular AMP (5). ZMP, which mimics AMP, also activates AMPK (6). AMPK is a heterotrimer composed of a catalytic α subunit and regulatory β and γ subunits (7). Phosphorylation of Thr^{172} in its activation loop of α subunit by upstream kinases, namely, LKB1 (8,9) and Ca^{2+}/calmodulin-dependent kinase kinase (10,11) can increase its kinase activity (12). Activated AMPK inhibits the synthesis of fatty acids, cholesterol, proteins and gluconeogenesis in hepatocytes (13–16). Phosphorylation of $Ser^{485/491}$ by protein kinase B is known to inhibit AMPK activity (17).

Hepatitis C virus infection suppresses cellular glucose uptake through down-regulation of cell surface expression

Correspondence
Kiyonao Sada, Division of Microbiology, Department of Pathological Sciences, Faculty of Medical Sciences, University of Fukui, 23-3 Matsuoka-Shimoaizuki, Eiheiji, Fukui, 910-1193, Japan.
Tel: +81 776 61 8323; email: ksada@u-fukui.ac.jp

Received 29 June 2011; revised 4 August 2011; accepted 21 August 2011.

List of Abbreviations: AICAR, 5-aminoimidazole-4-carboxamide 1-β-D-ribofuranoside; AMP, adenosine monophosphate; AMPK, AMP-activated protein kinase; compound C, 6-(4-[2-piperidin-1-yl-ethoxy])-phenyl)-3-pyridin-4-yl-pyrrazolo(1,5-a)-pyrimidine; GAPDH, glyceraldehyde-3-phosphate dehydrogenase; HCV, hepatitis C virus; LKB1, liver kinase B1; MOI, multiplicity of infection; NS3, non-structural protein 3; PRPP, phosphoribosyl pyrophosphate; ZMP, 5-aminoimidazole-4-carboxamide ribonucleotide; ZTP, 5-aminoimidazole 4-carboxamide ribonucleoside 5-triphosphate.

of glucose transporters (18). Our preliminary experiments demonstrated that HCV infection alters the expression of 5-aminoimidazole-4-carboxamide ribonucleotide formyltransferase/inosine monophosphate cyclohydrolase, which catalyzes ZMP in purine nucleotide synthesis. ZMP is known to mimic the activating effects of AMP on AMPK (6). We postulated that glucose usage and/or activation of AMPK might affect the infection and replication of HCV.

In this study, we have investigated HCV replication with different glucose concentrations in the culture medium, with treatment of cells with AMPK activators (AICAR, metformin) or with the AMPK inhibitor compound C in the cell culture medium.

MATERIALS AND METHODS

Cells

The Huh-7.5 cell line used in this study, a highly HCV-susceptible subclone of Huh7 cells, was a kind gift from Dr. C. M. Rice (Center for the Study of Hepatitis C, The Rockefeller University, New York, NY, USA) (19). The cells were propagated in Dulbecco's modified Eagle medium supplemented with 10% heat-inactivated FBS and 0.1 mM nonessential amino acids.

Viruses

The virus stock was prepared as described previously (20,21). The pFL-J6/JFH1 plasmid that encodes the entire viral genome of a chimeric strain of HCV-2a, J6/JFH1, was kindly provided by Dr. C. M. Rice. The HCV RNA genome was transcribed *in vitro* from pFL-J6/JFH1 and transfected to Huh-7.5 cells. The supernatant was harvested as a virus stock. In this study we used an adapted strain of the virus obtained by passaging the HCV genotype 2a, J6/JFH1, infected cells 47 times (20,22). Virus infection was performed at a MOI of three. Culture supernatants of uninfected cells were used as controls (mock preparation). Virus infectivity was measured by indirect immunofluorescence analysis as described previously (20).

Reagents

5-aminoimidazole-4-carboxamide 1-β-D-ribofuranoside and uridine were purchased from Sigma (St. Louis, MO, USA), compound C from Chemdea (Ridgewood, NJ, USA), metformin from Enzo Life Sciences (Plymouth Meeting, PA, USA) and Hoechst 33258 from Wako (Osaka, Japan).

Immunoblotting

Immunoblotting was essentially as described previously (23). Cells were solubilized in a lysis buffer (50 mM Tris-HCl, pH 7.4, 150 mM NaCl, 100 mM NaF, 0.1 mM Na_3VO_4, 10 mM EDTA, 1% Triton-X, and protease inhibitor cocktail [Sigma]). Cell debris was removed by centrifugation and resulted supernatants were diluted 1:2 (v/v) with 3×sampling buffer. Protein quantification was carried out using a bicinchoninic acid protein assay kit (Thermo Fisher Scientific, Rockford, IL, USA). Equal amounts of soluble proteins were subjected to SDS-PAGE and transferred onto a polyvinylidene difluoride transfer membrane (Millipore, Billerica, MA, USA). After blocking in 5% milk in TBST (25 mM Tris, pH 8.0, 150 mM NaCl, and 0.1% Tween 20), the blots were reacted with the respective primary antibodies. The primary antibodies used were anti-phospho-AMPKα (Thr172) monoclonal antibody (clone D79.5E, Cell Signaling Technology, Danvers, MA, USA), anti-AMPKα antibody (Cell Signaling Technology), anti-HCV core monoclonal antibody (clone C7–50, Thermo Fisher Scientific), anti-AMPKα antibody (Phospho-Ser$^{485/491}$) (anti-pAMPK [Ser485/491]) (GenScript, Piscataway, NJ, USA), and anti-HCV NS3 monoclonal antibody (Millipore). Horseradish peroxidase-conjugated goat anti-mouse IgG or goat anti-rabbit IgG (Jackson ImmunoResearch Laboratories, West Grove, PA, USA) were used as secondary antibodies. The respective protein bands were visualized by enhanced chemiluminescence (PerkinElmer, Waltham, MA, USA) (24,25). Protein loading was normalized by probing with anti-GAPDH monoclonal antibody (clone 6C5, Millipore).

Indirect immunofluorescence

Cells seeded in 96-well plates were infected with HCV at a MOI of 3.0 for 4 hr or left uninfected. The cells were incubated for 30 hr and fixed with cold methanol for 10 min at room temperature. After being washed with PBS twice, the cells were stained with anti-HCV core monoclonal antibody and visualized by using horseradish peroxidase-conjugated goat anti-mouse IgG (Bio-Rad Laboratories, Hercules, CA, USA) and the tyramide signal amplification cyanine 3 system (Perkin Elmer). Stained cell samples were examined by fluorescence microscopy (Olympus IX70 microscope system, Tokyo, Japan).

Statistical analysis

The one-tailed Student *t*-test was applied to evaluate the statistical significance of differences found. A P value of <0.05 was considered statistically significant.

RESULTS

Glucose shortage in the culture medium suppresses the replication of hepatitis C virus along with activation of adenosine monophosphate-activated protein kinase

Any virus requires an energy source for replication. We surmised that glucose shortage in the cell culture medium would have a harmful effect on energy metabolism in HCV-infected Huh-7.5 cells. We used Huh-7.5 cells and a J6/JFH1-derived, cell-adapted strain of HCV throughout this study. First, we examined the effect of alterations in glucose concentration in the cell culture medium on the replication of HCV. Reducing the glucose concentration from 4.5 to 1.0 g/L resulted in a significant decrease in HCV replication, as demonstrated by decreased virus infectivity in culture supernatants (Fig. 1a), and decreased production of HCV core protein (Fig. 1b, third panel). In order to estimate the intracellular energy status, we examined the kinase activity of AMPK by the immunoblotting of phosphorylated Thr^{172} in AMPK. Reducing the glucose concentration from 4.5 to 2.0 g/L resulted in a dramatic increase in phosphorylation of Thr^{172} in AMPK, suggesting that Huh-7.5 cells sensed poor nutrition when cultured with 2.0 g/L of glucose in the medium, irrespective of infection with HCV (Fig. 1b). Phosphorylation of $Ser^{485/491}$ of AMPK was not affected by infection with HCV (Fig. 1c). Phosphorylation of AMPK was not affected by infection with HCV, although almost all of the cells were infected in this experiment (Fig. 1d). These results demonstrate that glucose shortage in the cell culture medium suppresses replication of HCV along with activation of AMPK in Huh-7.5 cells. Glucose shortage activates AMPK regardless of HCV infection.

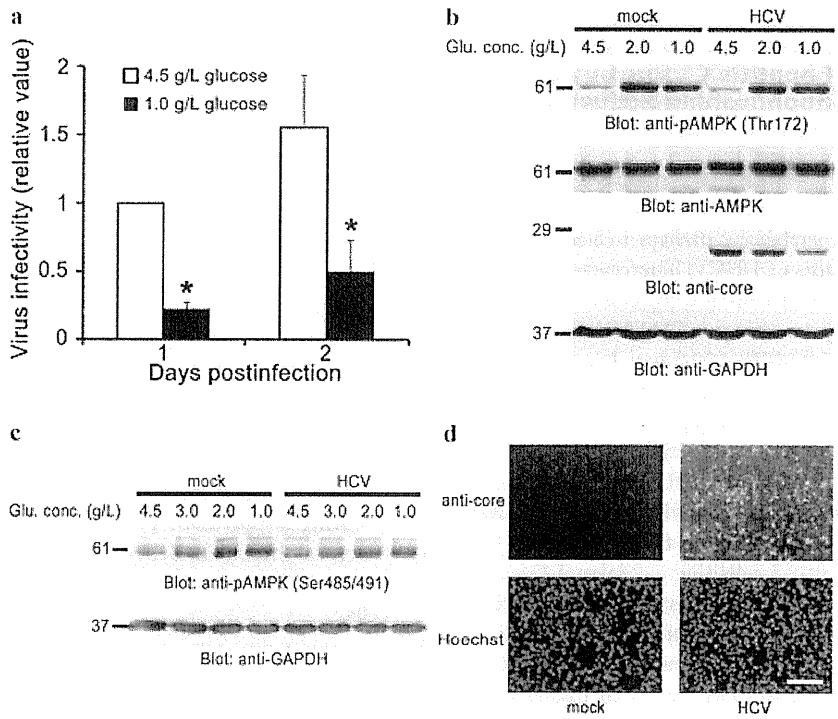

Fig. 1. Glucose shortage suppresses HCV replication and activates AMPK. (a) Huh-7.5 cells were infected with HCV at a MOI of 3.0 for 4 hr and then incubated at the indicated concentration of glucose in serum-free DMEM. Infectivity titer in culture supernatants of HCV-infected cells cultured in medium containing 4.5 g/L glucose at day 1 postinfection was arbitrarily expressed as 1.0. Data are expressed as means ± standard deviations (SD) of three independent experiments. *, $P < 0.05$, compared with the control. (b and c) Huh-7.5 cells were mock infected or infected with HCV at a MOI of 3.0 for 4 hr and then incubated at the indicated concentrations of glucose in serum-free DMEM for 30 hr. (b) Cell lysates were separated by SDS-PAGE and analyzed by immunoblotting with anti-phospho-AMPKα (Thr172) (anti-pAMPK (Thr172)), anti-AMPK, anti-HCV core, anti-GAPDH antibodies as indicated. (c) Cell lysates were analyzed by immunoblotting with anti-AMPKα antibody (anti-pAMPK (Ser485/491)) and anti-GAPDH monoclonal antibody. (d) Huh-7.5 cells mock infected or infected with HCV at a MOI of 3.0 for 4 hr were subjected to indirect immunofluorescence analysis by anti-HCV core antibody. Nuclei were stained with Hoechst 33258. Scale bar, 200 μm. Molecular size markers are indicated at the left in kilodaltons. The results are representative of three independent experiments. Conc., concentration; glu., glucose.

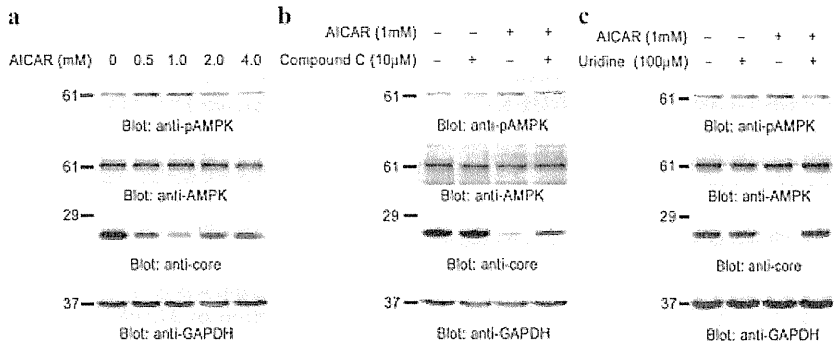

Fig. 2. AICAR suppresses HCV replication by activating AMPK. Huh-7.5 cells were infected with HCV at a MOI of 3.0 for 4 hr. (a) The cells were treated with the indicated concentrations of AICAR for 20 hr. (b) 10 μM compound C was added to the cells 30 min prior to the addition of AICAR and was present in the medium during the entire 20 hr of incubation with AICAR. (c) The cells were treated with 1 mM AICAR for 20 hr with or without supplementation with 100 μM uridine. Cell lysates were separated by SDS-PAGE and analyzed by immunoblotting as Figure 1. The results are representative of three independent experiments.

5-aminoimidazole-4-carboxamide 1-β-D-ribofuranoside suppresses the replication of hepatitis C virus by activating adenosine monophosphate-activated protein kinase in Huh-7.5 cells

Activated AMPK inhibits the synthesis of fatty acids, cholesterol, proteins and gluconeogenesis (13–16). Imbalance of these metabolic pathways in liver cells might affect the replication of HCV. Therefore we next examined whether activated AMPK suppresses the replication of HCV by using an activator (AICAR) and an inhibitor (compound C) of AMPK. Mankauri J. *et al.* have previously reported that treatment of Huh-7 parental cells with AICAR suppresses the replication of JFH-1 (26). In this study, we adopted a more efficient HCV replication system, Huh-7.5 cells and a J6/JFH1-derived, cell-adapted strain of HCV. Similar to the previous finding, activation of AMPK by AICAR suppressed the expression of HCV core protein in Huh-7.5 cells (Fig. 2a, lanes 1–3). Activation of AMPK by AICAR was observed when the cells were treated with relatively low concentrations (0.5 or 1.0 mM), but not with higher concentrations (2.0 or 4.0 mM). Possible reasons for the latter effect are that higher concentrations of AICAR could suppress the synthesis of purine nucleotides and/or increase the concentration of ZTP, thus inhibiting AMPK (6,27).

To examine whether the inhibitory effect of AICAR on HCV replication is mediated by activation of AMPK, we tested an AMPK inhibitor (compound C) in this experiment. We found that pretreatment of cells with 10 μM compound C attenuates AICAR-mediated suppression of HCV core protein expression (Fig. 2b, lane 4). This suggests that AICAR-mediated suppression of HCV replication is mediated by activation of AMPK. Addition of compound C to the cell culture medium without AICAR did not affect the expression of HCV core protein, suggesting that this inhibitor does not affect the replication of HCV under nutritious condition in which AMPK is inactive (Fig. 2b, lane 2).

In the presence of AICAR, the amounts of uridine triphosphate and cytidine triphosphate are decreased in the cultured cells as a result of PRPP depletion (27). PRPP is an important precursor for pyrimidine nucleotide synthesis. PRPP-derived pyrophosphate can increase ZTP/ZMP which are then no longer able to activate AMPK (6,28). To complement the pyrimidine shortage in Huh-7.5 cells treated with AICAR, the cells were co-incubated with 100 μM uridine in the presence of 1 mM AICAR. This resulted in the complete prevention of AICAR-mediated activation of AMPK and the resulting suppression of HCV (Fig. 2c, lane 4). Taken together, these data demonstrate that AICAR suppresses the replication of HCV by activating AMPK in Huh-7.5 cells.

Glucose shortage and metformin have an anti-hepatitis C virus effect independently of adenosine monophosphate-activated protein kinase activation

It is important to note that glucose shortage activates AMPK because of cellular energy limitations, whereas AICAR can activate AMPK regardless of cellular energy status. Therefore we tried another AMPK activator, metformin, which activates AMPK by impairing complex 1 of the mitochondrial respiratory chain (29,30). In addition, in mice metformin has a LKB1/AMPK-independent

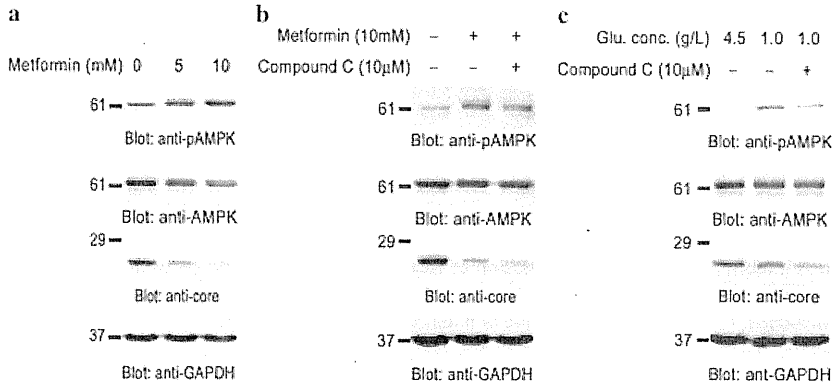

Fig. 3. Compound C, an AMPK inhibitor, stimulates the anti-HCV effects of glucose shortage or metformin. Huh-7.5 cells were infected with HCV at a MOI of 3.0 for 4 hr. (a) The cells were treated with the indicated concentration of metformin for 20 hr. (b) 10 μM compound C was added to the cells 30 min prior to the addition of metformin and present in the medium during the entire 20 hr of incubation with metformin. (c) The cells were incubated with or without 10 μM compound C at the indicated glucose concentrations in serum-free DMEM for 15 hr. Cell lysates were separated by SDS-PAGE and analyzed by immunoblotting as Figure 1. The results are representative of three independent experiments. Conc., concentration; glu., glucose.

inhibitory role on gluconeogenesis by decreasing the hepatic energy state (31). Treatment of cells with metformin activated AMPK and suppressed replication of HCV in a concentration-dependent manner in Huh-7.5 cells (Fig. 3a). However, co-incubation of cells with compound C, an inhibitor of AMPK, did not prevent metformin-mediated suppression of HCV replication (Fig. 3b, lane 3). Relatively speaking, compound C enhances the suppression of HCV replication induced by metformin. Likewise, compound C promoted suppression of HCV replication when the cells were cultured under conditions of glucose shortage (Fig. 3c, lane 3). These results demonstrate that glucose shortage and metformin inhibit HCV replication independently of AMPK activation.

The effects of adenosine monophosphate-activated protein kinase activators/inhibitor on hepatitis C virus non-structural protein 3

Finally, we tested the effects of AMPK activators/inhibitor on the expression of other HCV protein besides core protein (Fig. 4). As shown, treatment of cells with AICAR, metformin or glucose shortage suppressed the expression of NS3 protein. In addition, compound C attenuated the anti-HCV effect of AICAR, whereas it enhanced the anti-HCV effect of metformin or glucose shortage. These results support the conclusion that AMPK activators/inhibitor affect the replication of HCV, as demonstrated by the expression of HCV core protein (Figs. 1–3).

DISCUSSION

Previous reports have suggested that HCV infection directly causes insulin resistance, resulting in the progression of diabetes (32,33). Moreover it has been reported that insulin resistance is a negative predictor of the response to antiviral therapy in chronic hepatitis C patients treated with peginterferon plus ribavirin (4). However, the association between virus proliferation and hyperglycemia due to insulin resistance remains elusive. In this study, we have demonstrated that HCV proliferation is promoted in Huh-7.5 cells cultured at 4.5 g/L glucose, the equivalent of the blood glucose concentrations of diabetes patients (Fig. 1). This result suggests that intensive control of glucose concentrations would aid antiviral therapy in hepatitis C patients with diabetes.

We have demonstrated that activation of AMPK suppresses HCV replication (Fig. 2). This result suggests that AMPK as a potential target for the treatment of chronic hepatitis C. Therapeutic interest has recently been increased by the findings that hepatic AMPK is activated by adiponectin (34) and by thiazolidinedione-type antidiabetic drugs (35). Pharmacological activation of AMPK may provide a new strategy for both the management of chronic hepatitis C itself and metabolic hepatic disorders linked to HCV infection.

Adenosine monophosphate-activated protein kinase, a major energy sensor, is activated by energy depletion. AMPK is directly activated by AICAR, being metabolized to ZMP in the cell, regardless of the cellular energy status (6). We have demonstrated that AICAR-mediated suppression of HCV proliferation is AMPK-dependent

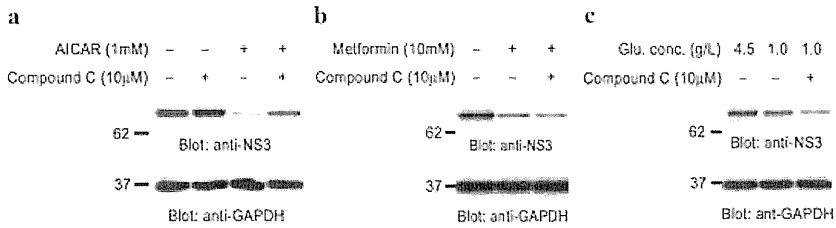

Fig. 4. AMPK activators/inhibitors' effect on the expression of HCV NS3 protein. Huh-7.5 cells were infected with HCV at a MOI of 3.0 for 4 hr. The cells were treated with the indicated reagents. Cell lysates were separated by SDS-PAGE and analyzed by immunoblotting with anti-HCV NS3 and anti-GAPDH antibodies. The results are representative of three independent experiments.

(Fig. 2). In terms of phosphorylation of AMPK, the most effective concentration of AICAR was 0.5 mM, whereas the most effective concentration of AICAR for suppression of HCV replication was clearly 1.0 mM. One of the possible explanations of this discrepancy is that the former immunoblot shows the state of AMPK phosphorylation at the endpoint of the experiment, whereas the latter immunoblot reflects the accumulation of the expression of core protein during the whole period of the experiment. Compound C, a specific AMPK inhibitor that competes with ATP (36), could inhibit the effect of AICAR on HCV proliferation (Fig. 2b). Compound C did not completely reverse the suppressive effect of AICAR treatment on HCV replication. In general, inhibitors do not completely suppress the effect of reagents or enzymes; however it is still possible that the suppression of HCV replication by AICAR cannot be explained purely by activation of AMPK. Uridine as a source of pyrimidine could also prevent the effect of AICAR (Fig. 2c). Moreover, we focused on another mechanism of AICAR-mediated inhibition of HCV replication. Activated AMPK causes inhibitions of fatty acids and cholesterol synthesis. Recent reports have shown a crucial involvement of fatty acids, cholesterol and lipid droplets in infectious virion production (37–40). Therefore, we predicted that AICAR-mediated inhibition of HCV replication might be due to lipid depletion. To investigate this possibility, we added mevalonolactone and/or oleic acid in the presence of AICAR to the cell culture medium, and then examined the replication of HCV. However, the addition of lipids had almost no effect on AICAR-mediated suppression of HCV (Fig. S1). This suggests that HCV replication does not require additional lipids when the cells are treated with AICAR, which shifts cellular metabolism from energy expenditure to energy production by activating AMPK.

Cell confluency is known to activate AMPK, and LKB1 is a major kinase that activates AMPK. Replication of the HCV replicon is known to be inhibited in confluent Huh-7 cells (41). Replication of HCV replicon in HeLa cells, a known LKB1-deficient cell line, is not affected by their confluence (42). These data suggest that confluence-mediated suppression of HCV replication requires the LKB1-AMPK pathway. Our experiments demonstrated that confluence of cells can activate AMPK and suppress replication of HCV in Huh-7.5 cells (Fig. S2). It is still not clear whether this anti-HCV effect is due to relative undernutrition resulting from increased cell numbers or the activation of AMPK by the confluence itself.

Culturing cells under a shortage of glucose or with metformin can activate cellular AMPK and suppress replication of HCV in the cells (Fig. 1 and 3). Under such low energy conditions, compound C, a specific AMPK inhibitor, can induce further suppression of HCV replication. The explanation of this phenomenon is as follows: AMPK is activated in order to restore energy status. In the presence of glucose depletion or energy limitations by metformin, compound C-induced AMPK inhibition may lead to failure to maintain ATP concentrations. Various compensatory mechanisms may maintain intracellular ATP concentrations. In other words, under energy limitations the breakdown of the fuel gauge, AMPK, may proceed to imbalance in metabolism leading to poor replication of HCV. Recent reports have shown that metformin therapy is associated with a reduced hepatocarcinogenesis risk in type 2 diabetes patients (43) and an improvement of sustained virological response in chronic hepatitis C patients (44). The present study provides evidence for the possibility that not only metformin monotherapy, but also AMPK inhibitor and metformin combination therapy, may be helpful in the treatment of chronic hepatitis C.

In a previous study using JFH-1 strain of HCV and Huh-7 cells, it was reported that HCV-infection causes $Ser^{485/491}$ phosphorylation of AMPK and inhibits the kinase activity of AMPK. Inhibition of AMPK facilitates HCV replication (26). In the present study using Huh-7.5 cells and a J6/JFH1-derived, cell-adapted strain of HCV, inhibition of AMPK by HCV replication was not observed. Moreover, phosphorylation of $Ser^{485/491}$ was not affected by HCV-infection (Fig. 1c). Since this experimental system using Huh-7.5 and the cell-adapted HCV strain produces

infectious HCV particles efficiently, inhibition of AMPK by HCV replication may play a minor role in efficient HCV replication. In addition, a previous study having shown that AMPK activators suppress HCV replication, we further investigated the mechanisms of AMPK involvement in HCV replication by using a specific AMPK inhibitor. AICAR-induced AMPK activation plays a critical role in the suppression of HCV (Fig. 2), meanwhile AMPK inhibitor rather potentiates the anti-HCV effects of metformin or glucose shortage (Fig. 3). These data suggest that AMPK activation does not simply lead to an anti-HCV effect.

In conclusion, we have shown the replication of HCV by AMPK-dependent and -independent mechanisms in Huh-7.5 cells. HCV does not replicate efficiently under the low energy conditions that activate AMPK. Hence, correction of hyperglycemia in hepatitis C patients should have a beneficial effect on anti-HCV therapy and the clinical course of hepatitis C. We suggest that AMPK is a therapeutic target for the treatment of chronic hepatitis C patients.

ACKNOWLEDGMENTS

The authors are grateful to Dr. C. M. Rice (The Rockefeller University, New York, NY, USA) for providing pFL-J6/JFH1 and Huh7.5 cells, to Dr. Takaji Wakita (National Institute of Infectious Diseases, Tokyo, Japan) for providing pSGR-JFH1 and to Ms. Satomi Nishibata and Ms. Kuniyo Miyagoshi for their assistance. This work was supported in part by Grant-in-Aids from the Japan Society for the Promotion of Science; the Ministry of Education, Culture, Sports, Science and Technology, Japan; the Ministry of Health, Labor and Welfare, Japan; JST/JICA SATREPS; the Yakult Foundation; and research grants from the University of Fukui, and Organization for Life Science Advancement Programs, University of Fukui.

DISCLOSURE

The authors who have taken part in this study declare that they do not have anything to disclose regarding funding or conflict of interest with respect to this manuscript.

REFERENCES

1. Manns M.P., Foster G.R., Rockstroh J.K., Zeuzem S., Zoulim F., Houghton M. (2007) The way forward in HCV treatment–finding the right path. *Nat Rev Drug Discov* **6**: 991–1000.
2. Inoue M., Kurahashi N., Iwasaki M., Tanaka Y., Mizokami M., Noda M., Tsugane S. (2009) Metabolic factors and subsequent risk of hepatocellular carcinoma by hepatitis virus infection status: a large-scale population-based cohort study of Japanese men and women (JPHC Study Cohort II). *Cancer Causes Control* **20**: 741–50.
3. Bressler B.L., Guindi M., Tomlinson G., Heathcote J. (2003) High body mass index is an independent risk factor for nonresponse to antiviral treatment in chronic hepatitis C. *Hepatology* **38**: 639–44.
4. Romero-Gomez M., Del Mar Viloria M., Andrade R.J., Salmeron J., Diago M., Fernandez-Rodriguez C.M., Corpas R., Cruz M., Grande L., Vazquez L., Munoz-De-Rueda P., Lopez-Serrano P., Gila A., Gutierrez M.L., Perez C., Ruiz-Extremera A., Suarez E., Castillo J. (2005) Insulin resistance impairs sustained response rate to peginterferon plus ribavirin in chronic hepatitis C patients. *Gastroenterology* **128**: 636–41.
5. Carling D., Clarke P.R., Zammit V.A., Hardie D.G. (1989) Purification and characterization of the AMP-activated protein kinase. Copurification of acetyl-CoA carboxylase kinase and 3-hydroxy-3-methylglutaryl-CoA reductase kinase activities. *Eur J Biochem* **186**: 129–36.
6. Corton J.M., Gillespie J.G., Hawley S.A., Hardie D.G. (1995) 5-aminoimidazole-4-carboxamide ribonucleoside. A specific method for activating AMP-activated protein kinase in intact cells? *Eur J Biochem* **229**: 558–65.
7. Dyck J.R., Gao G., Widmer J., Stapleton D., Fernandez C.S., Kemp B.E., Witters L.A. (1996) Regulation of 5'-AMP-activated protein kinase activity by the noncatalytic beta and gamma subunits. *J Biol Chem* **271**: 17798–803.
8. Hawley S.A., Boudeau J., Reid J.L., Mustard K.J., Udd L., Makela T.P., Alessi D.R., Hardie D.G. (2003) Complexes between the LKB1 tumor suppressor, STRAD alpha/beta and MO25 alpha/beta are upstream kinases in the AMP-activated protein kinase cascade. *J Biol* **2**: 28
9. Woods A., Johnstone S.R., Dickerson K., Leiper F.C., Fryer L.G., Neumann D., Schlattner U., Wallimann T., Carlson M., Carling D. (2003) LKB1 is the upstream kinase in the AMP-activated protein kinase cascade. *Curr Biol* **13**: 2004–8.
10. Hawley S.A., Pan D.A., Mustard K.J., Ross L., Bain J., Edelman A.M., Frenguelli B.G., Hardie D.G. (2005) Calmodulin-dependent protein kinase kinase-beta is an alternative upstream kinase for AMP-activated protein kinase. *Cell Metab* **2**: 9–19.
11. Woods A., Dickerson K., Heath R., Hong S.P., Momcilovic M., Johnstone S.R., Carlson M., Carling D. (2005) Ca2+/calmodulin-dependent protein kinase kinase-beta acts upstream of AMP-activated protein kinase in mammalian cells. *Cell Metab* **2**: 21–33.
12. Hawley S.A., Davison M., Woods A., Davies S.P., Beri R.K., Carling D., Hardie D.G. (1996) Characterization of the AMP-activated protein kinase kinase from rat liver and identification of threonine 172 as the major site at which it phosphorylates AMP-activated protein kinase. *J Biol Chem* **271**: 27879–87.
13. Munday M.R., Campbell D.G., Carling D., Hardie D.G. (1988) Identification by amino acid sequencing of three major regulatory phosphorylation sites on rat acetyl-CoA carboxylase. *Eur J Biochem* **175**: 331–8.
14. Clarke P.R., Hardie D.G. (1990) Regulation of HMG-CoA reductase: identification of the site phosphorylated by the AMP-activated protein kinase *in vitro* and in intact rat liver. *EMBO J* **9**: 2439–46.
15. Horman S., Browne G., Krause U., Patel J., Vertommen D., Bertrand L., Lavoinne A., Hue L., Proud C., Rider M. (2002) Activation of AMP-activated protein kinase leads to the phosphorylation of elongation factor 2 and an inhibition of protein synthesis. *Curr Biol* **12**: 1419–23.
16. Lochhead P.A., Salt I.P., Walker K.S., Hardie D.G., Sutherland C. (2000) 5-aminoimidazole-4-carboxamide riboside mimics the effects of insulin on the expression of the 2 key gluconeogenic genes PEPCK and glucose-6-phosphatase. *Diabetes* **49**: 896–903.